

SUPPLEMENTARY MATERIAL

New Mononuclear Cu(I) Compounds Synthesis, Characterization, and Application to the Electroreduction of CO₂.

Alma Arévalo, Enrique Juárez, Diego Roa, Marcos Flores-Alamo and Juventino J. García*

Index

- Figure S1.** ³¹P{¹H}(THF-d₈) NMR of Compound (2) [(dippe)Cu(PPh₃)NO₃].
- Figure S2.** ¹³C{¹H} (THF-d₈) NMR of Compound (2) [(dippe)Cu(PPh₃)NO₃]. Full spectra.
- Figure S3.** ¹³C{¹H} (THF-d₈) NMR of Compound (2) [(dippe)Cu(PPh₃)NO₃]. Aliphatic zone.
- Figure S4.** ¹³C{¹H} (THF-d₈) NMR of Compound (2). Aromatic zone-
- Figure S5.** ¹H (THF-d₈) NMR of Compound (2) [(dippe)Cu(PPh₃)NO₃].
- Figure S6.** ¹H (THF-d₈) NMR of Compound (2) [(dippe)Cu(PPh₃)NO₃]. Aromatic Zone.
- Figure S7.** IR-ATR (neat) of Compound (2) [(dippe)Cu(PPh₃)NO₃].
- Figure S8.** Elemental Analysis for Compound (2) [(dippe)Cu(PPh₃)NO₃].
- Figure S9.** ³¹P{¹H} (THF-d₈) NMR of Compound (3) [(depe)Cu(PPh₃)NO₃].
- Figure S10.** ¹H (THF-d₈) NMR of Compound (3) [(depe)Cu(PPh₃)NO₃].
- Figure S11.** ¹³C{¹H} (THF-d₈) NMR of Compound (3) [(depe)Cu(PPh₃)NO₃]. Full spectra.
- Figure S12.** ¹³C{¹H} (THF-d₈) NMR of Compound (3) [(depe)Cu(PPh₃)NO₃]. Aliphatic zone.
- Figure S13.** ¹³C{¹H} (THF-d₈) NMR of Compound (3) [(depe)Cu(PPh₃)NO₃]. Aromatic zone.
- Figure S14.** IR-ATR (neat) of Compound (3) [(depe)Cu(PPh₃)NO₃].
- Figure S15.** Elemental Analysis of Compound (3) [(depe)Cu(PPh₃)NO₃].

Figure S16. $^{31}\text{P}\{^1\text{H}\}$ (THF- d_8) NMR of Compound (4) [(dppe)Cu(PPh₃)NO₃].

Figure S17. ^1H NMR (THF- d_8) of Compound (4) [(dppe)Cu(PPh₃)NO₃].

Figure S18. IR-ATR (neat) of Compound (4) [(dppe)Cu(PPh₃)NO₃].

Figure S19. Elemental Analysis of Compound (4) [(dppe)Cu(PPh₃)NO₃].

Figure S20. $^{31}\text{P}\{^1\text{H}\}$ (THF- d_8) NMR of Compound (5), [(dipf)CuNO₃].

Figure S21. ^1H (THF- d_8) NMR of Compound (5), [(dipf)CuNO₃].

Figure S22. $^{13}\text{C}\{^1\text{H}\}$ (THF- d_8) NMR of Compound (5) [(dipf)CuNO₃].

Figure S23. IR-ATR (neat) of Compound (5), [(dipf)CuNO₃].

Figure S24. Elemental Analysis for Compound (5) [(dipf)CuNO₃].

Table S1. Crystal data and structure refinement for (2). [(dippe)Cu(PPh₃)(NO₃)]

Table S2. Bond lengths [Å] and angles [°] for (2) [(dippe)Cu(PPh₃)(NO₃)]

Table S3. Crystal data and structure refinement for (3) [(depe)Cu(PPh₃)(NO₃)]

Table S4. Bond lengths [Å] and angles [°] for (3) [(depe)Cu(PPh₃)(NO₃)]

Table S5. Crystal data and structure refinement for (5) [(dipf)Cu(NO₃)]

Table S6. Bond lengths [Å] and angles [°] for (5) [(dipf)Cu(NO₃)]

Table S7. Overpotential values (η) for the Cu(I) compounds.

Figure S25. CV trace for dry acetonitrile.

Figure S26. CV trace for dry acetonitrile and CO₂.

Figure S27. CV trace for ferrocene/ferrocinium pair.

Figure S28. Anodic peaks assignments corresponding to phosphine ligands in compound (2) [(dippe)Cu(PPh₃)NO₃].

Figure S29. Assignment of anodic peaks of the phosphine ligands for compound (3) [(depe)Cu(PPh₃)NO₃].

Figure S30. Assignment of anodic peaks of the phosphine ligands for compound (4) [(dppe)Cu(PPh₃)NO₃].

Figure S31. Assignment of anodic peaks of the phosphine ligands for compound (5) [(dipf)CuNO₃].

Figure S32. Compound (2) behavior with different scanning speeds in Ar atmosphere.

Figure S33. Pseudo-first-order behavior of the cathodic process of Compound (2)

Figure S34. Compound (2) behavior with different scanning speeds in CO₂ atmosphere.

Figure S35. Pseudo-first-order behavior of the cathodic process of Compound (2) with CO₂.

Figure S36. Compound (2) behavior with variable water equivalents under Ar atmosphere.

Figure S37. Compound (2) behavior with variable acetic acid equivalents under Ar and CO₂ atmosphere.

Figure S38. Compound (2) behavior with variable phenol equivalents and inhibition of the CO₂RR process.

Figure S39. Compound (2) behavior with variable benzoic acid equivalents under Ar and CO₂ atmosphere.

Figure S40. Compound (2) behavior with variable PTSA equivalents under Ar and CO₂ atmosphere.

Figure S41. Compound (2) behavior with variable PTSA equivalents and inhibition of the CO₂RR process.

Figure S42. Compound (1) under Ar and CO₂ atmosphere.

Figure S43. Compound (1) [Cu(PPh₃)₂NO₃] behavior with variable phenol equivalents under Ar and CO₂ atmosphere.

Figure S44. Compound (1) behavior with variable benzoic acid equivalents under Ar and CO₂ atmosphere.

Figure S45. Compound (1) behavior with variable water equivalents under Ar and CO₂ atmosphere.

Figure S46. Compound (1) behavior with variable PTSA equivalents under Ar and CO₂ atmosphere.

Figure S47. Compound (1) behavior with variable PTSA equivalents and inhibition of the CO₂RR process.

Figure S48. Compound (1) behavior with variable acetic acid equivalents under Ar and CO₂ atmosphere.

Figure S49. Compound (3) under Ar and CO₂ atmosphere.

Figure S50. Compound (3) behavior with variable acetic acid equivalents under Ar and CO₂ atmosphere.

Figure S51. Compound (3) behavior with variable PTSA equivalents under Ar and CO₂ atmosphere.

Figure S52. Compound (3) behavior with variable phenol equivalents under Ar and CO₂ atmosphere.

Figure S53. Compound (3) behavior with variable benzoic acid equivalents under Ar and CO₂ atmosphere.

Figure S54. Compound (3) behavior with variable water equivalents under Ar and CO₂ atmosphere.

Figure S55. Compound (4) under Ar and CO₂ atmosphere.

Figure S56. Compound (4) behavior with variable PTSA equivalents under Ar and CO₂ atmosphere.

Figure S57. Compound (4) behavior with variable phenol equivalents under Ar and CO₂ atmosphere.

Figure S58. Compound (4) behavior with variable benzoic acid equivalents under Ar and CO₂ atmosphere.

Figure S59. Compound (4) behavior with variable water equivalents under Ar and CO₂ atmosphere.

Figure S60. Compound (4) behavior with variable acetic acid equivalents under Ar and CO₂ atmosphere.

Figure S61. Compound (5) under Ar and CO₂ atmosphere.

Figure S62. Compound (5) behavior with variable PTSA equivalents under Ar and CO₂ atmosphere.

Figure S63. Compound (5) behavior with variable phenol equivalents under Ar and CO₂ atmosphere.

Figure S64. Compound (5) behavior with variable benzoic acid equivalents under Ar and CO₂ atmosphere.

Figure S65. Compound (5) behavior with variable water equivalents under Ar and CO₂ atmosphere.

Figure S66. Compound (5) behavior with variable acetic acid equivalents under Ar and CO₂ atmosphere.

Figure S67. Elemental analysis of [Rh(PPh₃)₃Cl(NO)].

Figure S68. MS spectra of hydrolyzed product (d).

Spectroscopic Data for the Obtained Compounds

Compound (2), [(dippe)Cu(PPh₃)NO₃].

Compound (2). NMR (600 MHz): ³¹P{¹H} (THF-d₈), δ=0.45 ppm (br. s., PPh₃), δ=12.14 ppm (br. s., dippe). ¹³C{¹H} δ= 20.21 ppm (s, -CH₃), δ= 20.53 ppm (s, -CH₂- bridge), δ= 25.18 ppm (s, -CH-*i*Pr), δ= 129.7 ppm (d, *m*-PPh₃, ³J_{C-P}= 7.5 Hz), δ= 130.6 ppm (s, *p*-PPh₃), δ= 135.5 ppm (d, *o*-C-PPh₃, ²J_{C-P}= 15.09 Hz), δ= 137.81 ppm (s, ⁱC-PPh₃).

^1H , $\delta=1.20$ ppm (s, $-\text{CH}_3$), $\delta=1.91$ ppm (s, $-\text{CH}_2-$ bridge), $\delta=2.15$ ppm (s, $-\text{CH}$ -isopropyl), $\delta=7.37$ ppm (m, H_o y H_m $-\text{PPh}_3$), $\delta=7.54$ ppm (t, H_p $-\text{PPh}_3$). IR (ATR-neat): 3055 cm^{-1} , 2954 cm^{-1} , 2868 cm^{-1} (w, $\text{C}=\text{C}$ $-\text{PPh}_3$ ring), 1399 cm^{-1} (s, $\text{N}-\text{O}$ sym), 1299 cm^{-1} (s, $\text{N}-\text{O}$ asym.), 700 cm^{-1} (s, $-\text{PPh}_3$ ring). Anal. Calcd. for : $\text{C}_{32}\text{H}_{47}\text{O}_3\text{NP}_3\text{Cu}$: %C, 59.11, %H, 7.3, %N, 2.15. Found: %C, 56.9, %H, 7.5, %N: 2.3. Melting point: $202\text{ }^\circ\text{C}$ (d).

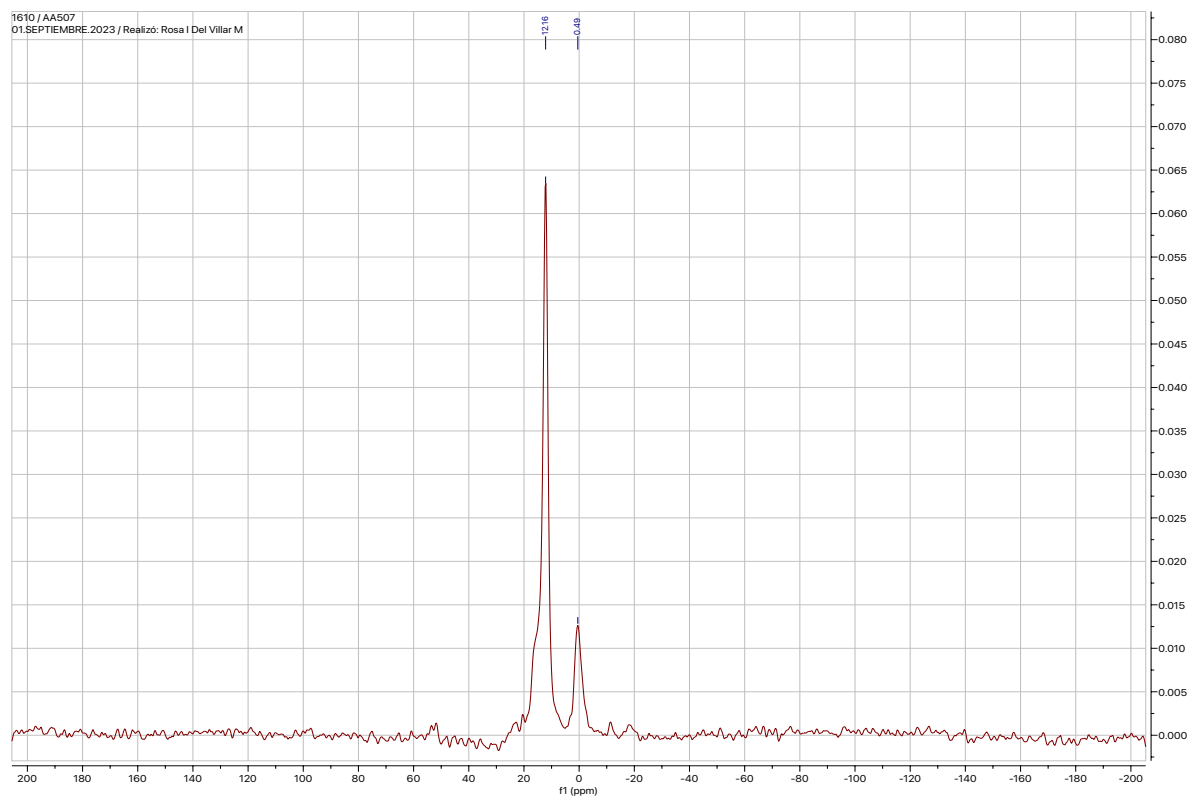
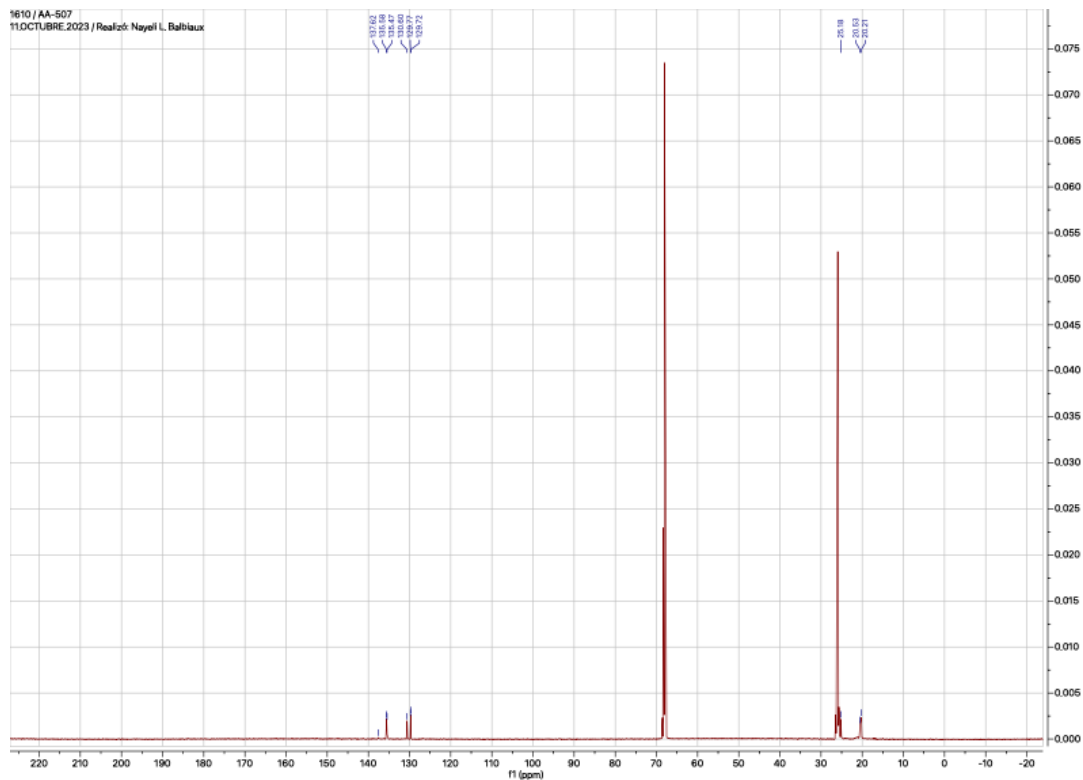


Figure S1. $^{31}\text{P}\{^1\text{H}\}$ (THF- d_8) NMR of Compound (2),



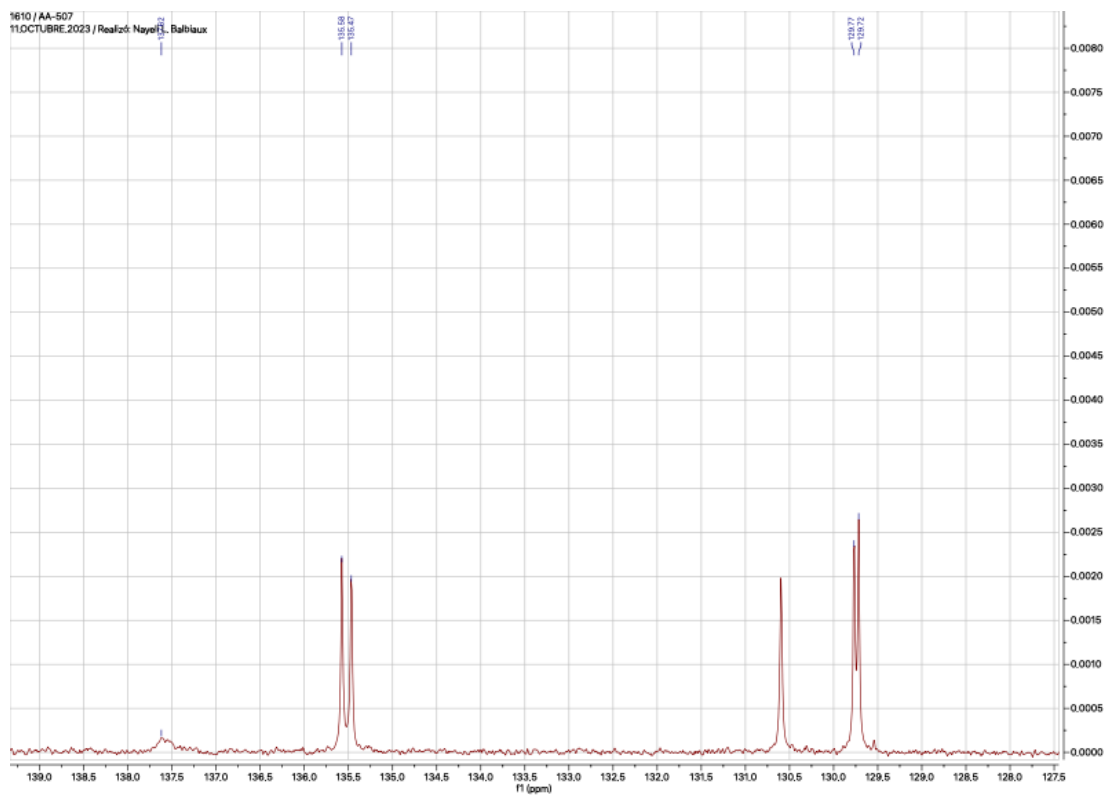


Figure S4. $^{13}\text{C}\{^1\text{H}\}$ (THF- d_8) NMR of Compound (**2**). Aromatic zone-

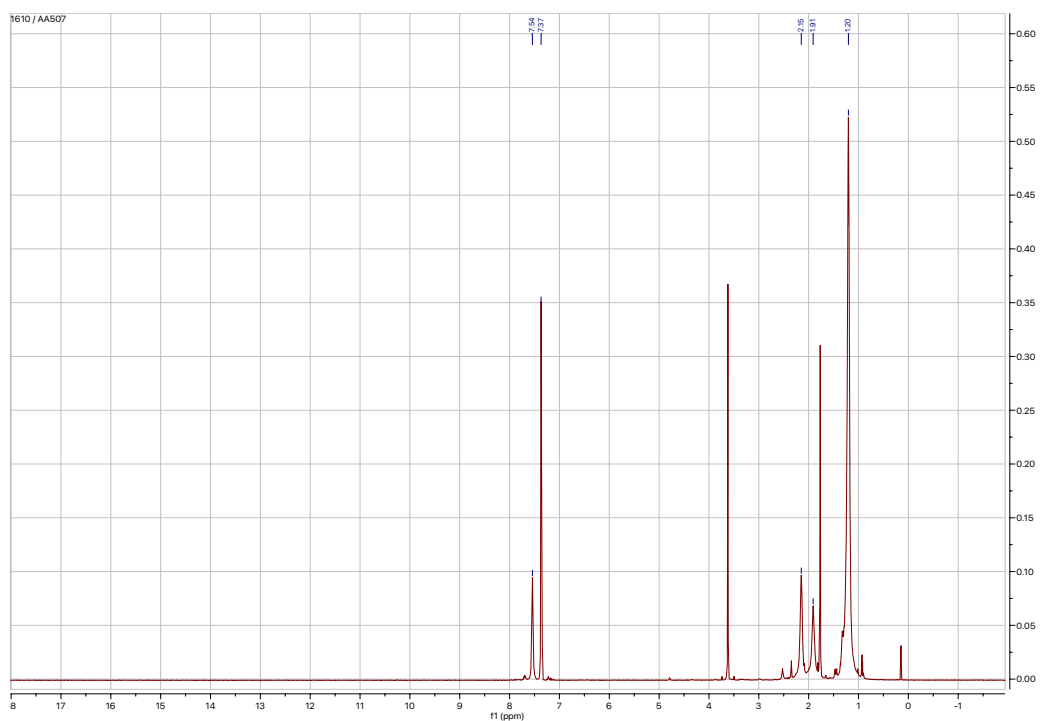


Figure S5. ^1H NMR (THF- d_8) NMR of Compound (**2**)

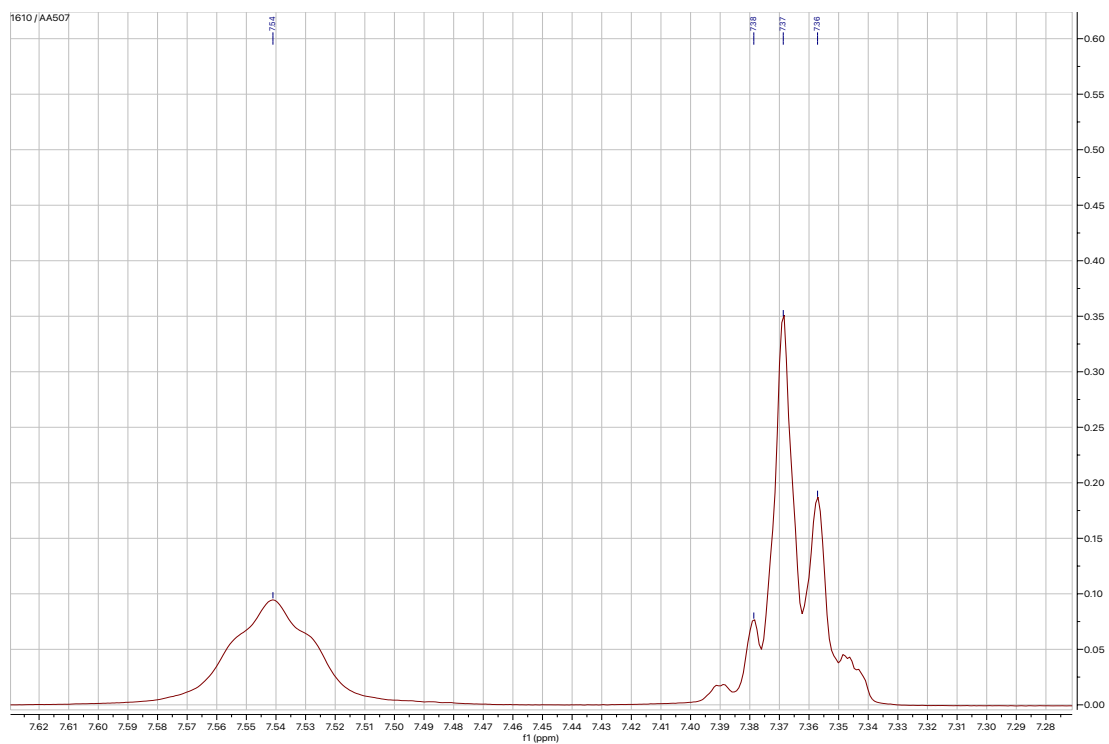


Figure S6. ¹H NMR (THF-d₈) NMR of Compound (2) Aromatic Zone.

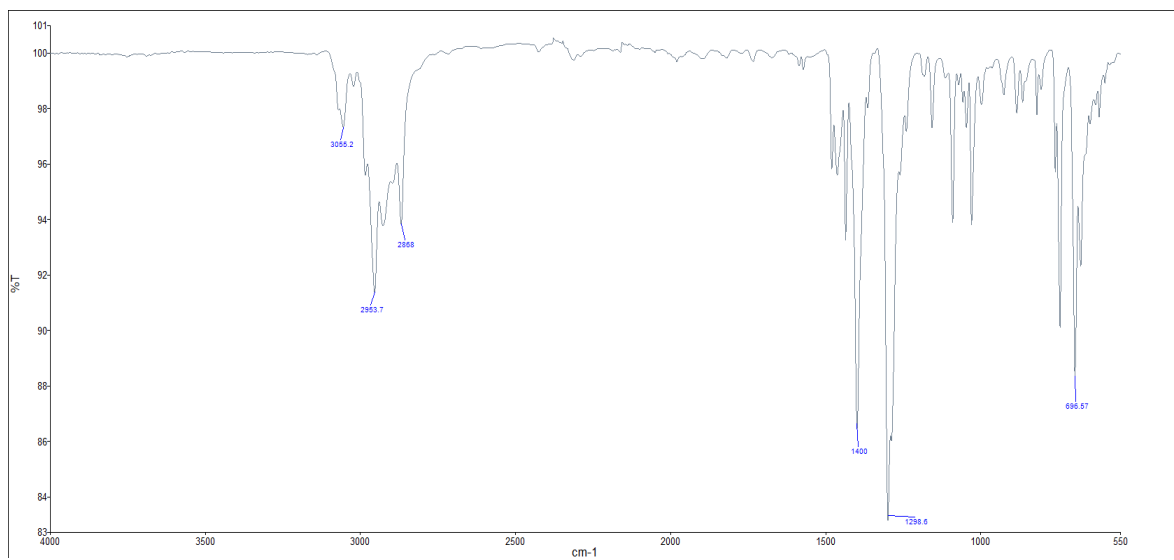


Figure S7. IR-ATR (neat) of Compound (2) [(dippe)Cu(PPh₃)NO₃].

| | |
|-----------------------|-----------------------------------------|
| Date of report | 25-Oct-22 6:13:44PM |
| User ID | Realizo: M en I. Victor Hugo Lemus Neri |
| Comments | Muestra: AA507 |

| Run | Weight | Carbon | Hydrogen | Nitrogen | Created on |
|-------------|--------------------|--------|----------|----------|----------------------|
| 1414826104A | 1.128 | 55.68% | 7.49% | 2.32% | 25-Oct-22 3:05:18 PM |
| 1414826104B | 1.56 | 58.16% | 7.55% | 2.4% | 25-Oct-22 3:10:10 PM |
| | Average | 56.920 | 7.520 | 2.360 | |
| | Variance | 3.075 | 0.002 | 0.003 | |
| | Standard Deviation | 0.305 | 1.754 | 0.042 | 0.057 |

Figure S8. Elemental Analysis for Compound (2)

Compound (3). [(depe)Cu(PPh₃)NO₃]

Compound (3). NMR (600MHz): ³¹P{¹H} (THF-d₈): δ=-6.47 (d, P-bridge), δ= 2.78 ppm (m, -PPh₃). ¹H: δ= 0.95 ppm (m, -CH₃), δ= 1.60 ppm (s, -CH₂), δ=2.52 ppm (m, -CH₂ bridge), δ= 7.3 ppm (2H, -PPh₃), δ= 7.37 ppm (2H, -PPh₃), δ= 7.51 ppm (H, PPh₃). IR (ATR-neat): 3053-2875 cm⁻¹(-CH₃ and -CH₂-, str.), 1434 cm⁻¹(N-O asym), 1337 cm⁻¹ (C-H felx.), 1090-1028 cm⁻¹ (C-H arom.), 694 cm⁻¹ (C-H arom.). Anal. Calcd. for C₂₈H₃₉O₃NP₃Cu: %C, 56.7, %H, 6.62, %N, 2.3. Found: %C, 62, %H, 6.6, %N, 2.02. Melting point: 257 °C (d).

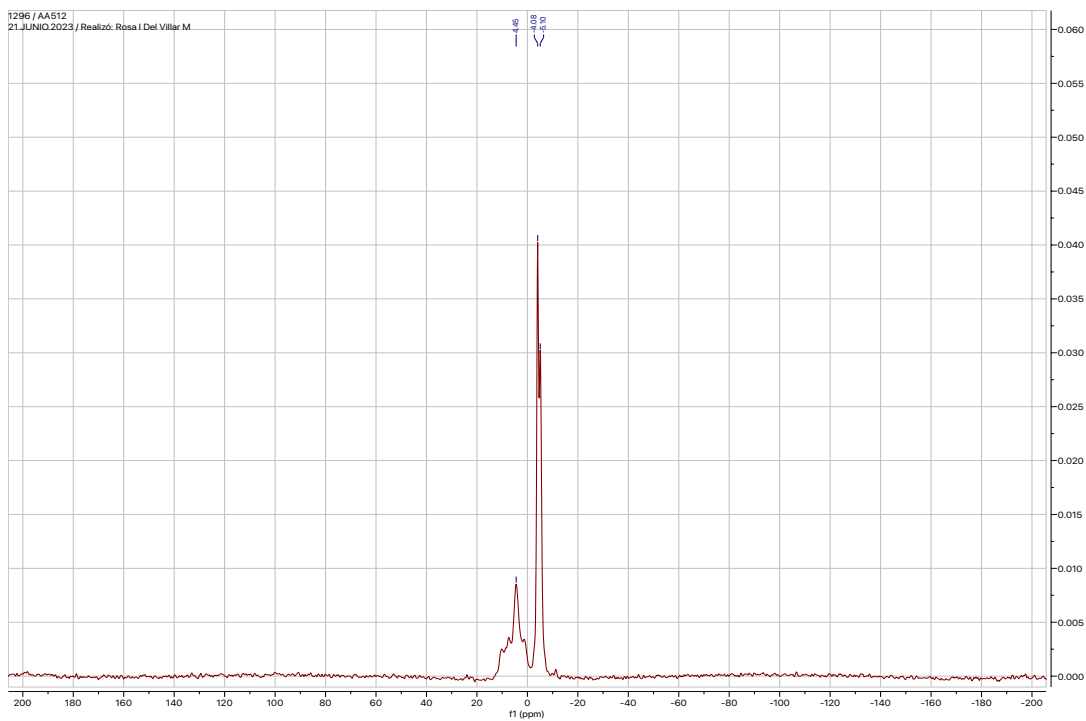


Figure S9. $^{31}\text{P}\{^1\text{H}\}$ (THF- d_8) NMR of Compound **(3)** [(depe)Cu(PPh $_3$)NO $_3$].

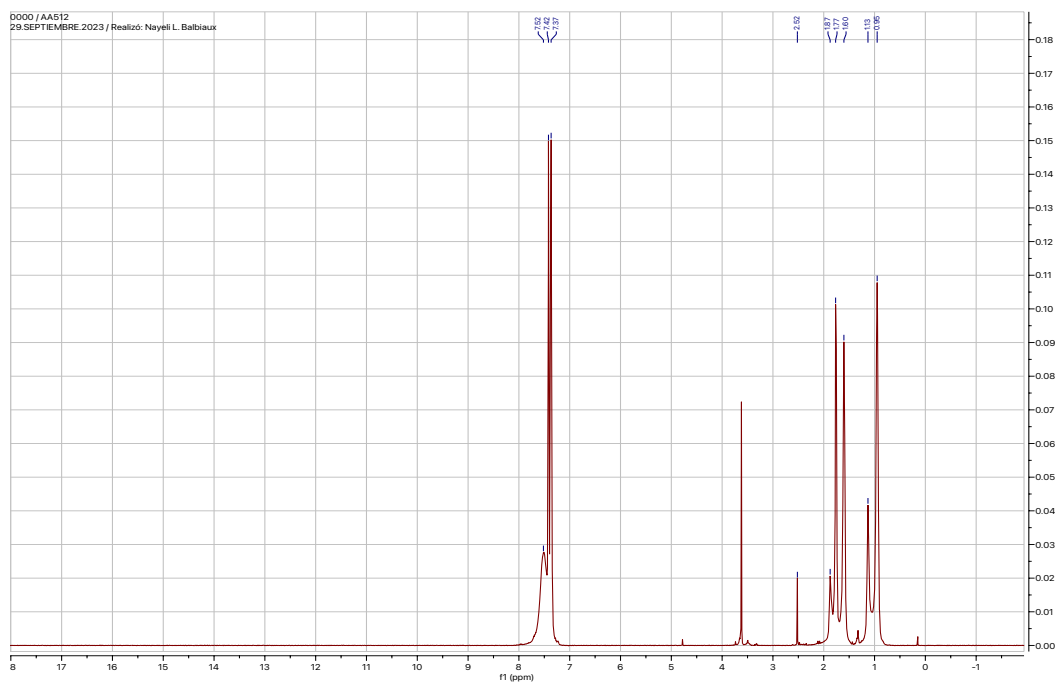


Figure S10. ^1H (THF- d_8) NMR of Compound **(3)** [(depe)Cu(PPh $_3$)NO $_3$].

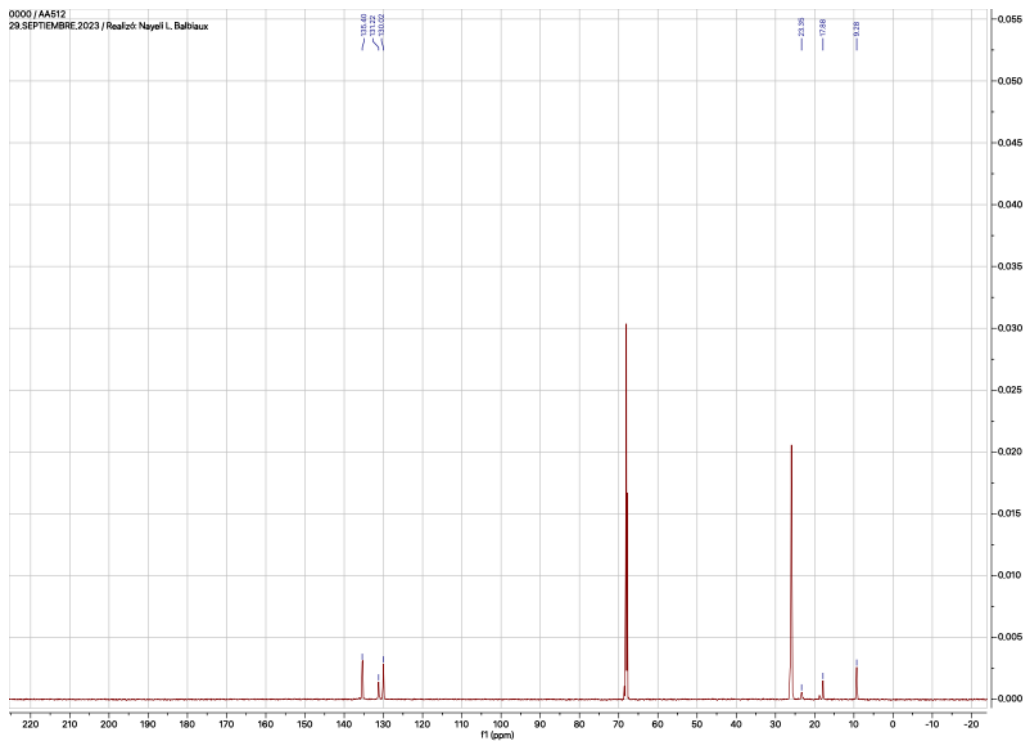


Figure S11. $^{13}\text{C} \{^1\text{H}\}$ (THF- d_8) NMR of Compound (**3**). Full spectra.

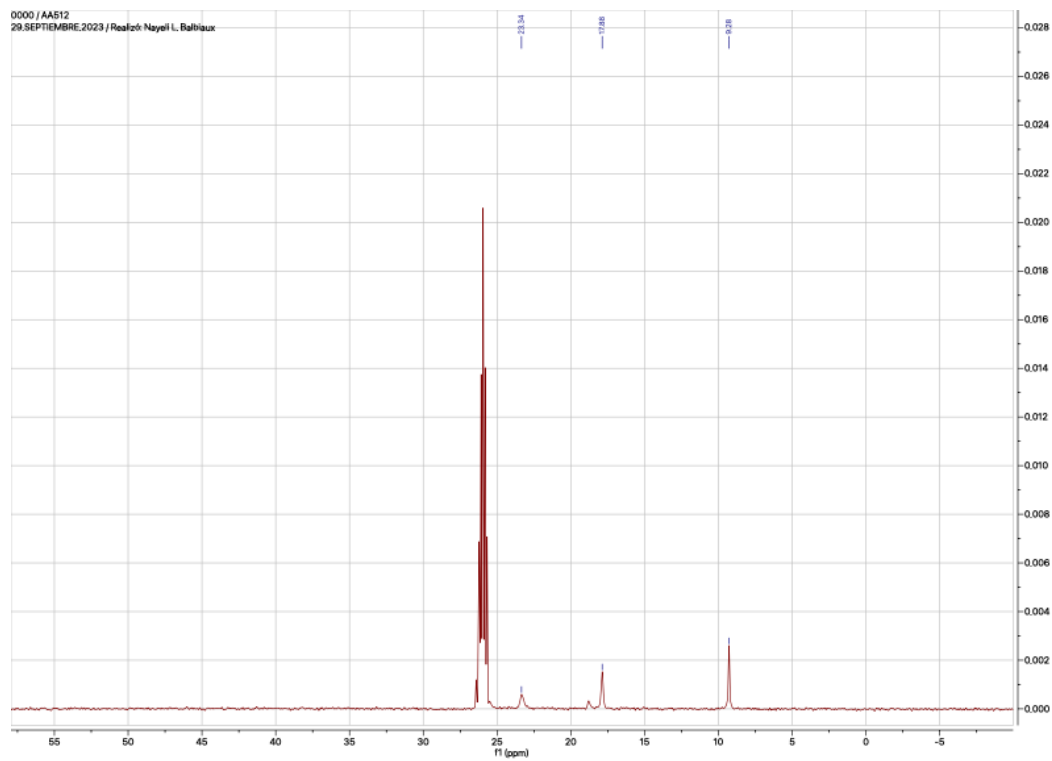


Figure S12. $^{13}\text{C} \{^1\text{H}\}$ (THF- d_8) NMR of Compound (**3**) Alifatic zone.

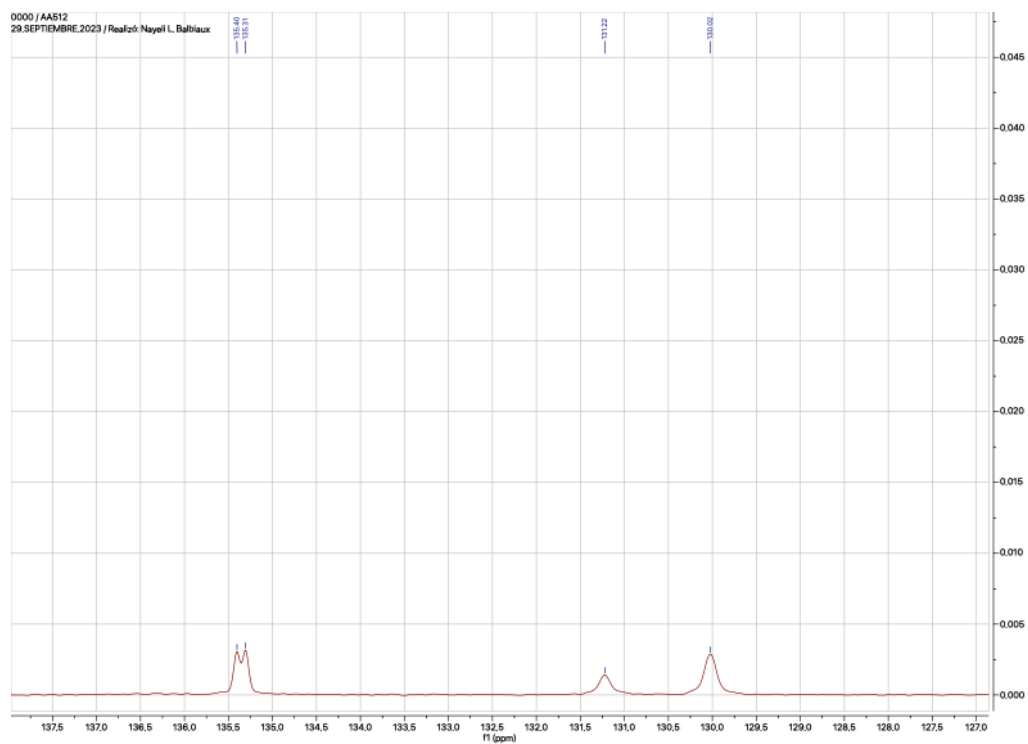


Figure S13. $^{13}\text{C} \{^1\text{H}\}$ (THF- d_8) NMR of Compound (**3**) Aromatic zone.

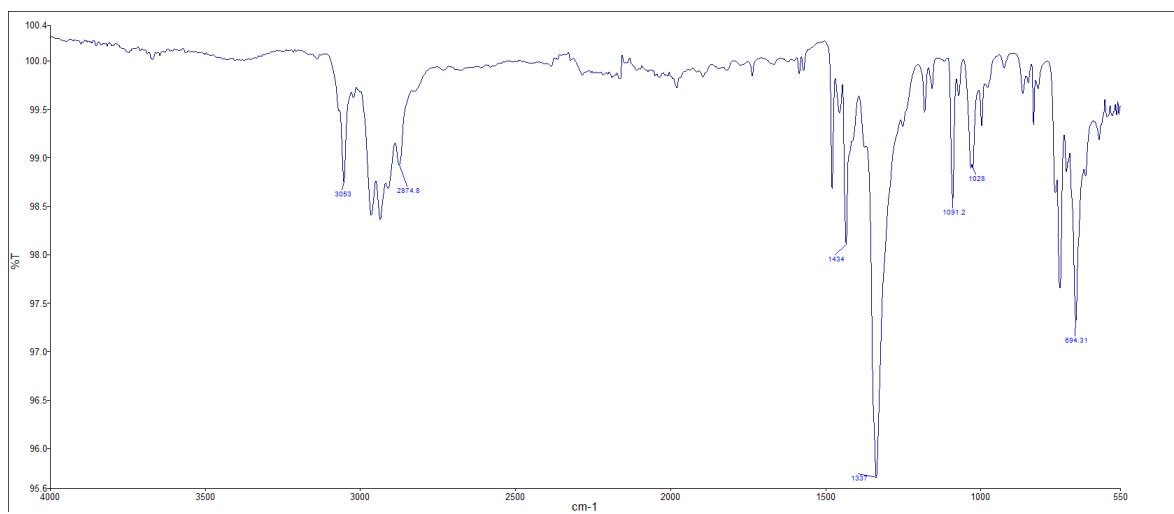


Figure S14. IR-ATR (neat) of Compound (**3**) [(depe)Cu(PPh₃)NO₃].

| | | | | | |
|-----------------------|-----------------------------------------|--------|----------|----------|----------------------|
| Date of report | 21-Jun-23 12:33:30PM | | | | |
| User ID | Realizo: M en I, Victor Hugo Lemus Neri | | | | |
| Comments | Muestra: AAS12 | | | | |
| Run | Weight | Carbon | Hydrogen | Nitrogen | Created on |
| 1789770720B | 2.28 | 62.51% | 6.75% | 2.02% | 20-Jun-23 2:44:47 PM |
| 1789770720A | 2.187 | 62.19% | 6.61% | 2.02% | 20-Jun-23 2:39:40 PM |
| | Weight | Carbon | Hydrogen | Nitrogen | |
| Average | 2.234 | 62.350 | 6.680 | 2.020 | |
| Variance | 0.004 | 0.051 | 0.010 | 0.000 | |
| Standard Deviation | 0.066 | 0.226 | 0.099 | 0.000 | |

Figure S15. Elemental Analysis of Compound (3)

Compound (4). [(dppe)Cu(PPh₃)NO₃].

Compound (4). NMR (600MHz): ³¹P{¹H} (THF-d₈): δ=-6.22 ppm (s, P-bridge), δ=2.91 ppm (m, -PPh₃). ¹H: δ= 2.42 ppm (m, -CH bridge), δ= 7.3 ppm (m, aromatic phosphines). IR (ATR-neat): 3052 cm⁻¹ (C-H str. Arom.), 1434 cm⁻¹ (N-O asym), 1274 cm⁻¹ (N-O sym), 1096-1022 cm⁻¹ (C-H arom.), 692 cm⁻¹ (C-H arom.). Anal. Calcd. for C₄₄H₄₃O₃NP₃Cu: %C, 66.8, %H, 5.4, %N, 1.8. Found: %C, 66.8, %H, 5.1, %N, 2.6. Melting point: 256 °C (d).

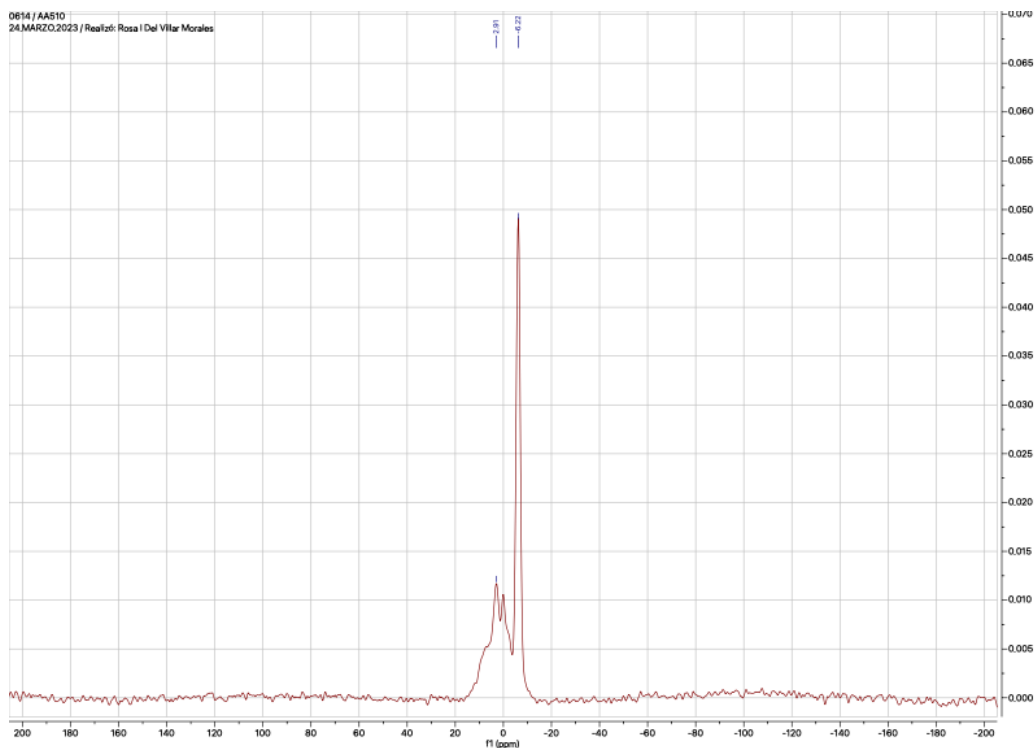


Figure S16 $^{31}\text{P}\{^1\text{H}\}$ (THF- d_8): NMR of Compound (4)

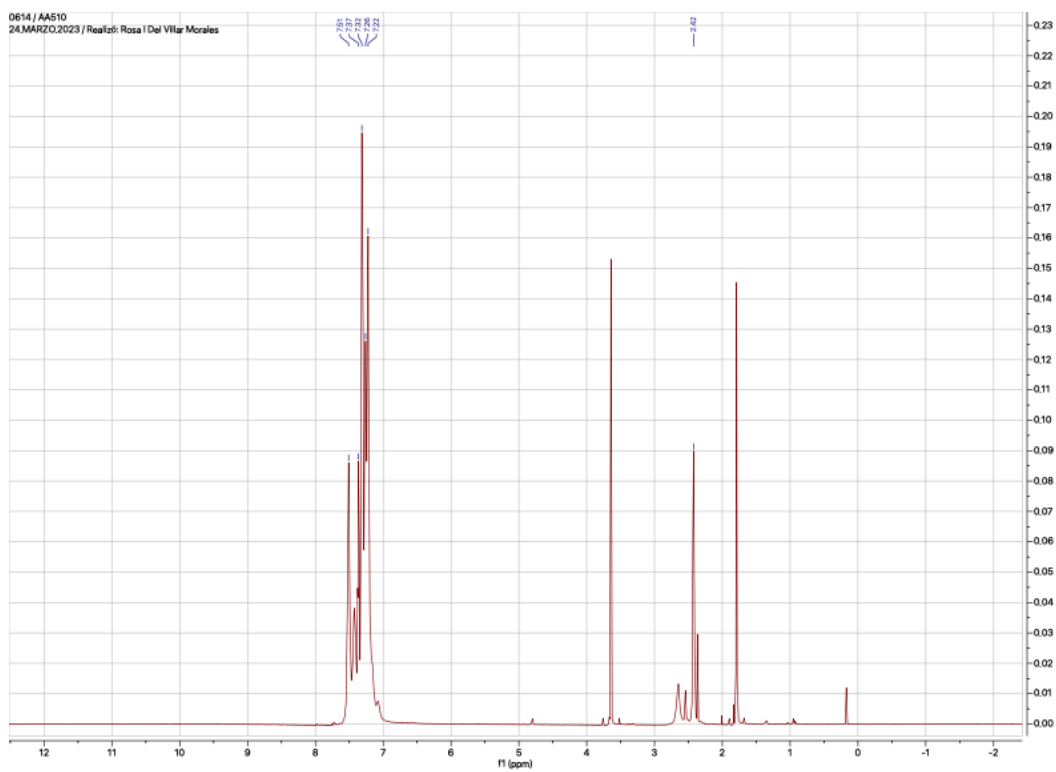


Figure S17. ^1H (THF- d_8): NMR of Compound (4)

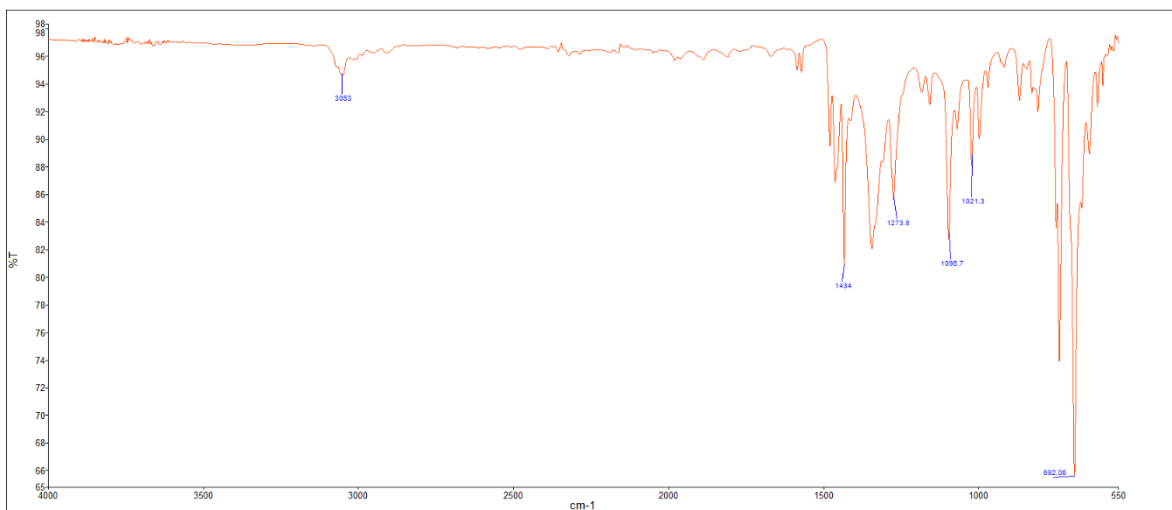


Figure S18. IR-ATR (neat) of Compound (4)

Unidad de Servicios de Apoyo a la Investigación y a la Industria (USAII)
 Facultad de Química, UNAM, Edificio H "Mario Molina"
 Email: vicemus@unam.mx
 Phone: 56.22.38.99 Ext. 84040

| | |
|-----------------------|-----------------------------------------|
| Date of report | 22-May-23 7:04:52PM |
| User ID | Realizo: M en I. Victor Hugo Lemus Neri |
| Comments | Muestra: AA510 |

| Run | Weight | Carbon | Hydrogen | Nitrogen | Created on |
|-------------|--------------------|--------|----------|----------|----------------------|
| 7734833569B | 1.227 | 66.79% | 5.14% | 2.72% | 22-May-23 4:39:04 PM |
| 7734833569A | 1.499 | 66.85% | 5.1% | 2.59% | 22-May-23 4:34:00 PM |
| | Weight | Carbon | Hydrogen | Nitrogen | |
| | Average | 66.820 | 5.120 | 2.655 | |
| | Variance | 0.002 | 0.001 | 0.008 | |
| | Standard Deviation | 0.0192 | 0.042 | 0.028 | |

Figure S19. Elemental Analysis of Compound (4).

Compound (5) [(dipf)CuNO₃].

Compound (5). NMR (600 MHz): ³¹P{¹H} (THF-d₈), δ= 3.13 ppm (s). ¹H, δ= 1.30 ppm (m, -CH₃), δ= 2.29 ppm (m, -CH-), δ= 4.44 (s, -CH, Fc), δ= 4.53 ppm (s, -CH, Fc). ¹³C{¹H}, δ= 20.59 ppm (m, -CH₃), δ= 21.44 ppm (-CH-), δ= 72.48 ppm (-CH-, Fc), δ= 75.19 ppm (-CH-, Fc). IR (ATR-neat): 2958-2866 cm⁻¹ (-C-H alkyl), 1431 cm⁻¹ (N-O asym), 1286 cm⁻¹ (N-O sym), 1024 cm⁻¹(Fc), 820 cm⁻¹ (Fc). Anal. Calcd. for C₂₂H₃₆O₃NP₂FeCu: %C,48.59, %H, 6.67, %N, 2.58. Found: %C, 50.22, %H, 6.81, %N, 3.11 Melting Point: 183 °C (d).

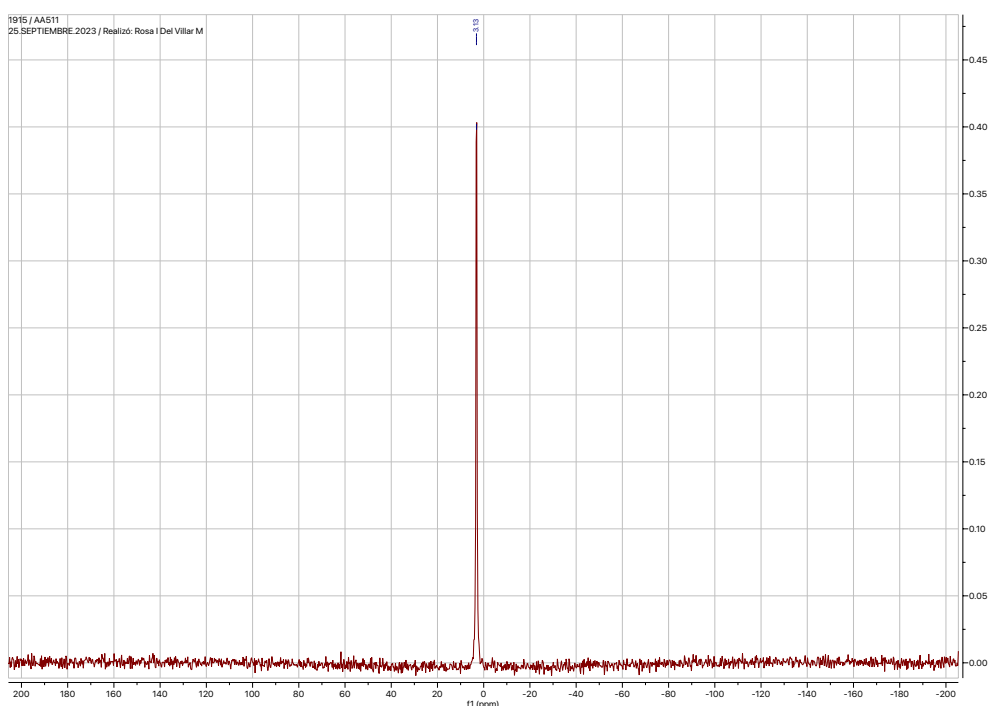


Figure S20. ³¹P{¹H} (THF-d₈) NMR of Compound (5).

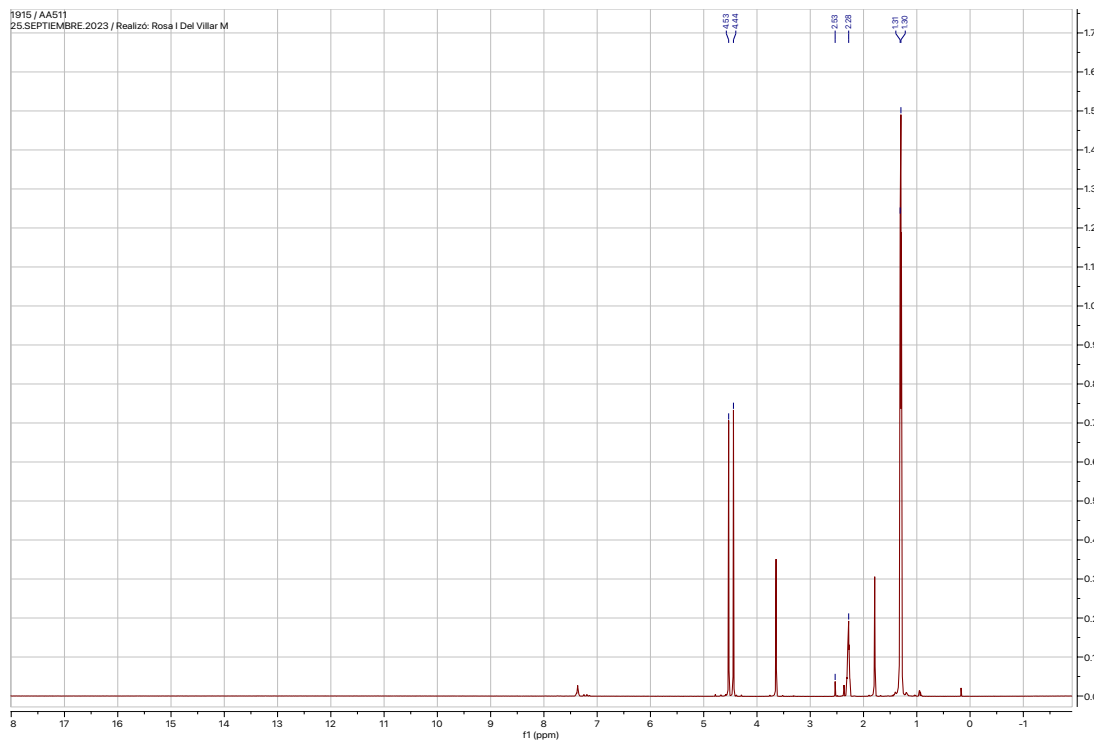


Figure S21. ^1H (THF- d_8) NMR of Compound (**5**),

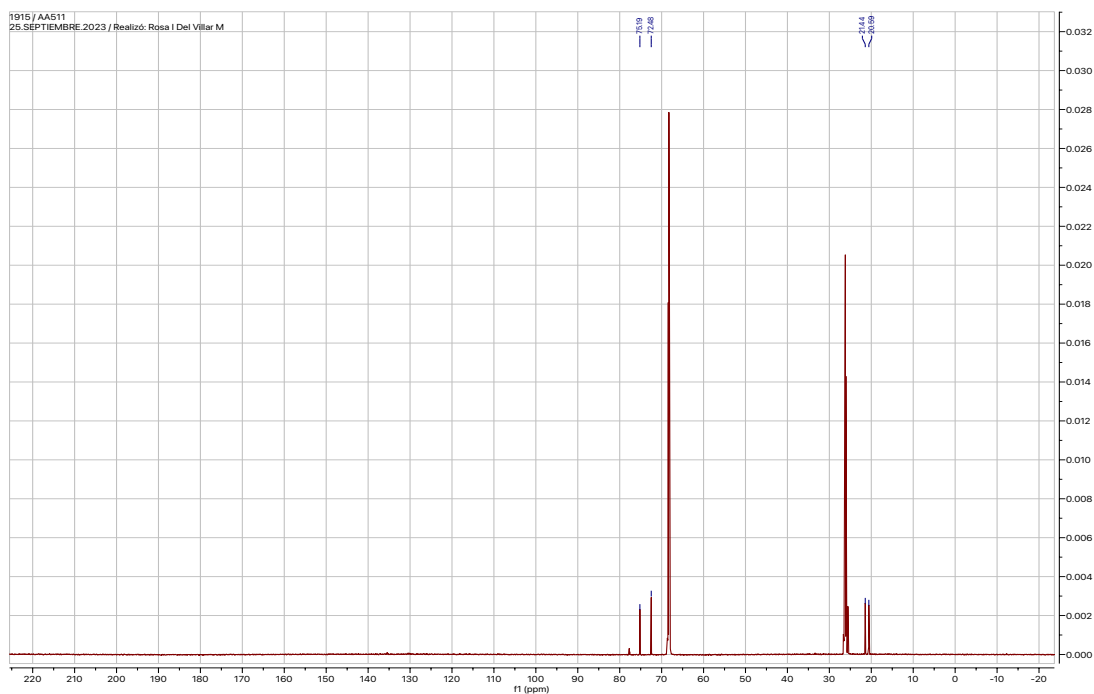


Figure S22. $^{13}\text{C}\{^1\text{H}\}$ (THF- d_8) NMR of Compound (**5**).

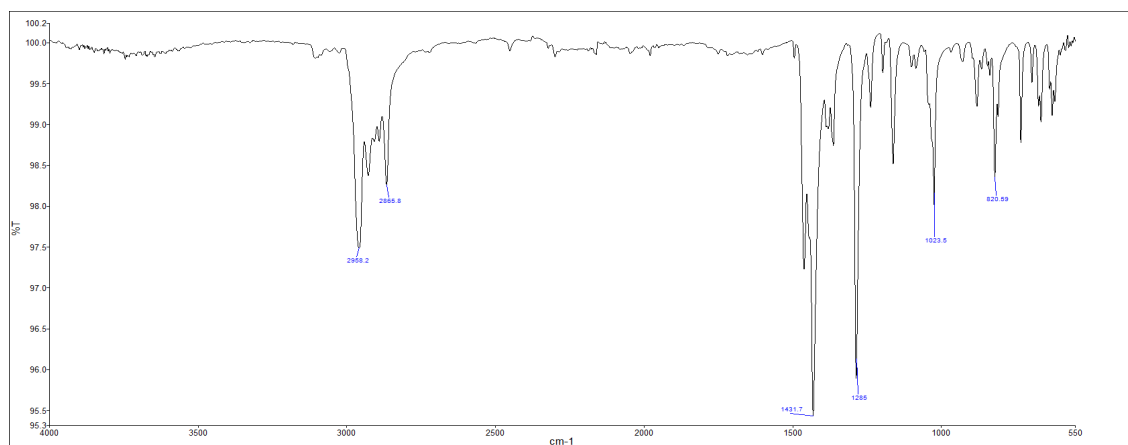


Figure S23. IR-ATR (neat) of Compound (5).

Unidad de Servicios de Apoyo a la Investigación y a la Industria (USAII)
 Facultad de Química, UNAM, Edificio H "Mario Molina"
 Email: viclemus@unam.mx
 Phone: 56.22.38.99 Ext. 84040

| | |
|-----------------------|-----------------------------------------|
| Date of report | 22-May-23 7:38:32PM |
| User ID | Realizo: M en I. Victor Hugo Lemus Neri |
| Comments | Muestra: AA511 |

22-May-23

| Run | Weight (mg) | Carbon | Hydrogen | Nitrogen |
|-------------|-------------|--------|----------|----------|
| 2846988985A | 1.439 | 50.22% | 6.81% | 3.11% |

Figure S24 Elemental Analysis for Compound (5).

XRD data for Cu(I) compounds

Table S1. Crystal data and structure refinement for (2) [(dippe)Cu(PPh₃)(NO₃)]

| Identification code | 2 | |
|-----------------------------------|--------------------------------------------------------------------|------------------------------------------|
| Empirical formula | C ₃₂ H ₄₇ Cu N O ₃ P ₃ | |
| Formula weight | 650.15 | |
| Temperature | 130(2) K | |
| Wavelength | 0.71073 Å | |
| Crystal system | Monoclinic | |
| Space group | P 21/n | |
| Unit cell dimensions | a = 12.7674(5) Å b = 17.7058(7) Å c = 15.0682(6) Å | α = 90°. β = 105.218(4)°. γ = 90°. |
| Volume | 3286.8(2) Å ³ | |
| Z | 4 | |
| Density (calculated) | 1.314 Mg/m ³ | |
| Absorption coefficient | 0.843 mm ⁻¹ | |
| F(000) | 1376 | |
| Crystal size | 0.400 x 0.370 x 0.270 mm ³ | |
| Theta range for data collection | 3.434 to 29.596°. | |
| Index ranges | -17 ≤ h ≤ 12, -24 ≤ k ≤ 15, -17 ≤ l ≤ 19 | |
| Reflections collected | 16174 | |
| Independent reflections | 7717 [R(int) = 0.0278] | |
| Completeness to theta = 25.242° | 99.7 % | |
| Refinement method | Full-matrix least-squares on F ² | |
| Data / restraints / parameters | 7717 / 0 / 369 | |
| Goodness-of-fit on F ² | 1.036 | |
| Final R indices [I > 2σ(I)] | R1 = 0.0539, wR2 = 0.1289 | |
| R indices (all data) | R1 = 0.0722, wR2 = 0.1436 | |
| Largest diff. peak and hole | 1.857 and -0.896 e.Å ⁻³ | |

Table S2. Selected bond lengths [Å] and angles [°] for **(2)** [(dippe)Cu(PPh₃)(NO₃)]

| | | | |
|-------------|-----------|------------------|------------|
| C(1)-C(2) | 1.510(5) | O(1)-Cu(1)-P(3) | 97.27(7) |
| C(1)-P(1) | 1.842(4) | O(1)-Cu(1)-P(2) | 111.01(7) |
| C(3)-C(5) | 1.500(6) | P(3)-Cu(1)-P(2) | 124.54(3) |
| C(3)-C(4) | 1.517(6) | O(1)-Cu(1)-P(1) | 108.62(7) |
| C(3)-P(1) | 1.868(4) | P(3)-Cu(1)-P(1) | 125.08(3) |
| C(15)-C(16) | 1.386(5) | P(2)-Cu(1)-P(1) | 90.25(3) |
| C(15)-P(3) | 1.828(3) | O(3)-N(1)-O(2) | 119.8(3) |
| Cu(1)-O(1) | 2.146(2) | O(3)-N(1)-O(1) | 119.2(3) |
| Cu(1)-P(3) | 2.2688(9) | O(2)-N(1)-O(1) | 121.0(3) |
| Cu(1)-P(2) | 2.2904(9) | C(1)-P(1)-C(6) | 104.7(2) |
| Cu(1)-P(1) | 2.2944(9) | C(15)-P(3)-Cu(1) | 116.01(11) |
| N(1)-O(3) | 1.251(4) | | |
| N(1)-O(2) | 1.253(4) | | |
| N(1)-O(1) | 1.254(4) | | |

Table S3. Crystal data and structure refinement for **(3)** [(depe)Cu(PPh₃)(NO₃)]

| Identification code | (3) | |
|-----------------------------------|--------------------------------------------------------------------|----------|
| Empirical formula | C ₂₈ H ₃₉ Cu N O ₃ P ₃ | |
| Formula weight | 594.05 | |
| Temperature | 130(2) K | |
| Wavelength | 0.71073 Å | |
| Crystal system | Orthorhombic | |
| Space group | P 21 21 21 | |
| Unit cell dimensions | a = 10.4119(11) Å | α = 90°. |
| | b = 15.363(2) Å | β = 90°. |
| | c = 18.5644(17) Å | γ = 90°. |
| Volume | 2969.5(6) Å ³ | |
| Z | 4 | |
| Density (calculated) | 1.329 Mg/m ³ | |
| Absorption coefficient | 0.926 mm ⁻¹ | |
| F(000) | 1248 | |
| Crystal size | 0.290 x 0.190 x 0.060 mm ³ | |
| Theta range for data collection | 3.474 to 29.616°. | |
| Index ranges | -14 ≤ h ≤ 14, -21 ≤ k ≤ 19, -22 ≤ l ≤ 24 | |
| Reflections collected | 16522 | |
| Independent reflections | 7018 [R(int) = 0.0646] | |
| Completeness to theta = 25.242° | 99.6 % | |
| Refinement method | Full-matrix least-squares on F ² | |
| Data / restraints / parameters | 7018 / 0 / 329 | |
| Goodness-of-fit on F ² | 1.088 | |
| Final R indices [I > 2σ(I)] | R1 = 0.0535, wR2 = 0.0674 | |
| R indices (all data) | R1 = 0.0934, wR2 = 0.0821 | |
| Absolute structure parameter | -0.017(13) | |
| Largest diff. peak and hole | 0.585 and -0.637 e.Å ⁻³ | |

Table S4. Selected bond lengths [Å] and angles [°] for **(3)** [(depe)Cu(PPh₃)(NO₃)]

| | | | |
|-------------|------------|------------------|------------|
| C(1)-C(2) | 1.537(7) | O(1)-Cu(1)-P(3) | 99.13(10) |
| C(1)-P(1) | 1.828(6) | O(1)-Cu(1)-P(2) | 109.20(11) |
| C(3)-C(4) | 1.532(7) | P(3)-Cu(1)-P(2) | 129.28(6) |
| C(3)-P(1) | 1.841(5) | O(1)-Cu(1)-P(1) | 112.16(11) |
| C(15)-C(16) | 1.391(7) | P(3)-Cu(1)-P(1) | 116.47(6) |
| C(15)-P(3) | 1.822(5) | P(2)-Cu(1)-P(1) | 90.84(5) |
| Cu(1)-O(1) | 2.090(3) | O(2)-N(1)-O(3) | 120.9(5) |
| Cu(1)-P(3) | 2.2323(13) | O(2)-N(1)-O(1) | 120.7(5) |
| Cu(1)-P(2) | 2.2593(16) | O(3)-N(1)-O(1) | 118.4(5) |
| Cu(1)-P(1) | 2.2759(16) | C(1)-P(1)-C(3) | 104.4(3) |
| N(1)-O(2) | 1.230(5) | C(6)-P(1)-C(3) | 104.0(3) |
| N(1)-O(3) | 1.237(5) | C(12)-P(2)-C(2) | 102.0(3) |
| N(1)-O(1) | 1.273(5) | C(12)-P(2)-C(9) | 105.1(3) |
| | | C(15)-P(3)-C(21) | 102.6(2) |

Table S5. Crystal data and structure refinement for (5) [(dipf)Cu(NO₃)]

| Identification code | (5) | |
|-----------------------------------|-----------------------------------------------------------------------|--------------------------------------------------------|
| Empirical formula | C ₂₂ H ₃₆ Cu Fe N O ₃ P ₂ | |
| Formula weight | 543.85 | |
| Temperature | 130(2) K | |
| Wavelength | 0.71073 Å | |
| Crystal system | Triclinic | |
| Space group | P -1 | |
| Unit cell dimensions | a = 8.6246(7) Å b = 9.3841(6) Å c = 17.1248(10) Å | α = 91.601(5)°. β = 97.997(6)°. γ = 100.216(6)°. |
| Volume | 1348.77(16) Å ³ | |
| Z | 2 | |
| Density (calculated) | 1.339 Mg/m ³ | |
| Absorption coefficient | 1.465 mm ⁻¹ | |
| F(000) | 568 | |
| Crystal size | 0.160 x 0.130 x 0.080 mm ³ | |
| Theta range for data collection | 3.568 to 29.590°. | |
| Index ranges | -11 ≤ h ≤ 11, -13 ≤ k ≤ 12, -23 ≤ l ≤ 23 | |
| Reflections collected | 29144 | |
| Independent reflections | 6766 [R(int) = 0.0493] | |
| Completeness to theta = 25.242° | 99.7 % | |
| Refinement method | Full-matrix least-squares on F ² | |
| Data / restraints / parameters | 6766 / 0 / 279 | |
| Goodness-of-fit on F ² | 1.032 | |
| Final R indices [I > 2σ(I)] | R1 = 0.0335, wR2 = 0.0646 | |
| R indices (all data) | R1 = 0.0512, wR2 = 0.0722 | |
| Largest diff. peak and hole | 0.493 and -0.370 e.Å ⁻³ | |

Table S6. Selected bond lengths [Å] and angles [°] for **(5)** [(dipf)Cu(NO₃)]

| | | | |
|-------------|------------|-------------------|------------|
| C(3)-C(5) | 1.534(3) | O(1)-Cu(1)-P(1) | 122.00(5) |
| C(3)-C(4) | 1.537(3) | O(1)-Cu(1)-P(2) | 113.29(4) |
| C(6)-P(1) | 1.852(2) | P(1)-Cu(1)-P(2) | 117.96(2) |
| C(9)-P(2) | 1.8553(19) | O(1)-Cu(1)-O(2) | 58.44(6) |
| C(12)-P(2) | 1.859(2) | P(1)-Cu(1)-O(2) | 117.31(4) |
| C(15)-C(16) | 1.436(3) | P(2)-Cu(1)-O(2) | 114.09(5) |
| C(15)-P(2) | 1.816(2) | C(19)-Fe(1)-C(23) | 140.20(8) |
| C(20)-C(21) | 1.444(3) | C(19)-Fe(1)-C(21) | 139.37(8) |
| C(20)-P(1) | 1.812(2) | C(15)-Fe(1)-C(16) | 40.79(8) |
| Cu(1)-O(1) | 2.1598(15) | O(3)-N(1)-O(2) | 122.0(2) |
| Cu(1)-P(1) | 2.2305(6) | O(3)-N(1)-O(1) | 121.3(2) |
| Cu(1)-P(2) | 2.2383(6) | O(2)-N(1)-O(1) | 116.70(18) |
| Cu(1)-O(2) | 2.2580(16) | C(6)-P(1)-C(3) | 106.05(9) |
| N(1)-O(3) | 1.239(2) | C(9)-P(2)-C(12) | 103.59(9) |
| N(1)-O(2) | 1.264(2) | | |
| N(1)-O(1) | 1.271(2) | | |

Table S7. Overpotential values (η) for the Cu(I) compounds-

| Compound | η_{NHE} (V) |
|----------|-------------------------|
| Cu-1 | 0.348 |
| Cu-2 | 0.39 |
| Cu-3 | 0.35 |
| Cu-4 | 0.30 |
| Cu-5 | 0.43 |

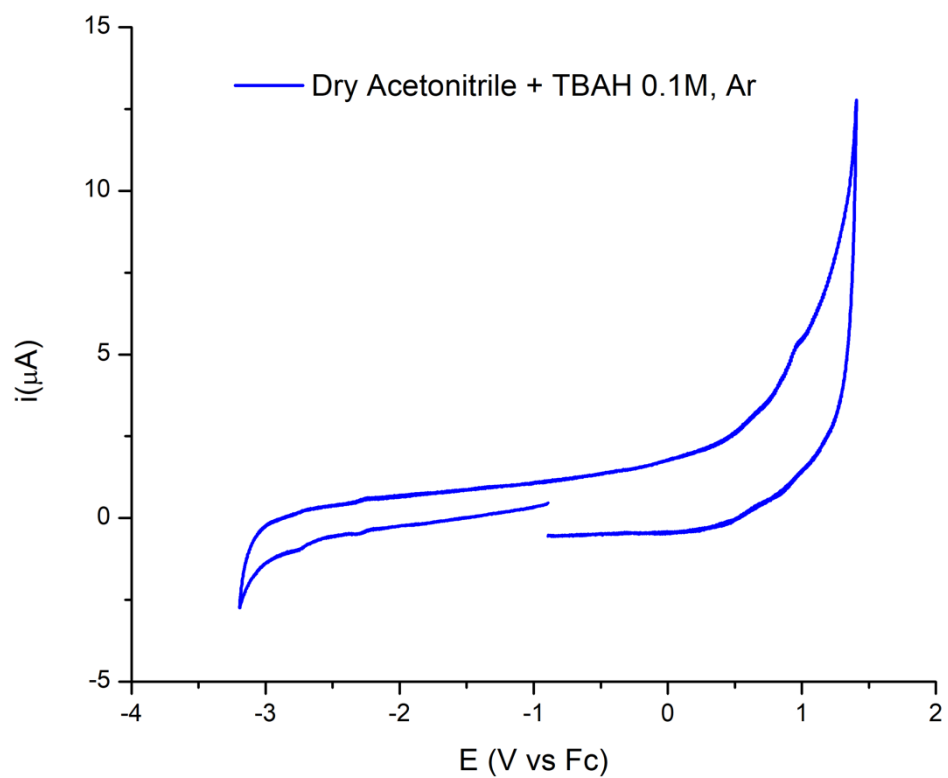


Figure S25. CV trace for dry acetonitrile.

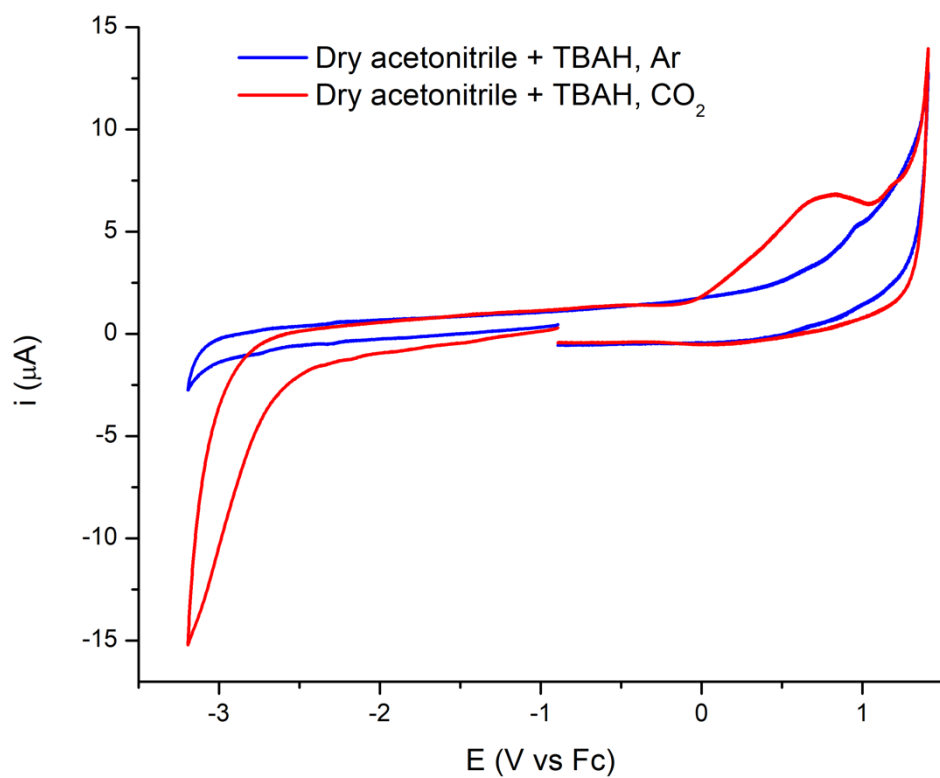


Figure S26. CV trace for dry acetonitrile and CO_2 .

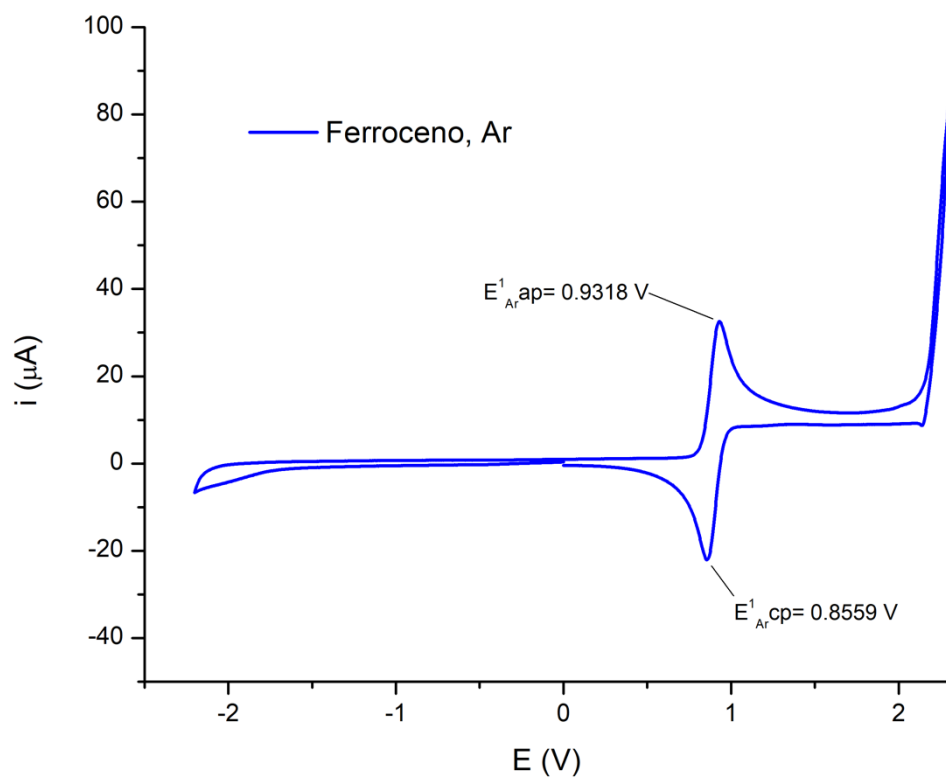


Figure S27. CV trace for ferrocene/ferrocinium pair.

Electrochemical Data for Cu(I) compounds.

ANODIC PEAKS ASSIGNMENT OF PHOSPHINES FOR Cu(I) COMPOUNDS

For compound (**2**), anodic peaks L1 were assigned to the oxidation process corresponding to dippe ligand while anodic peak L2 corresponds to the sum of PPh₃ oxidation and to the second oxidation process for dippe ligand.

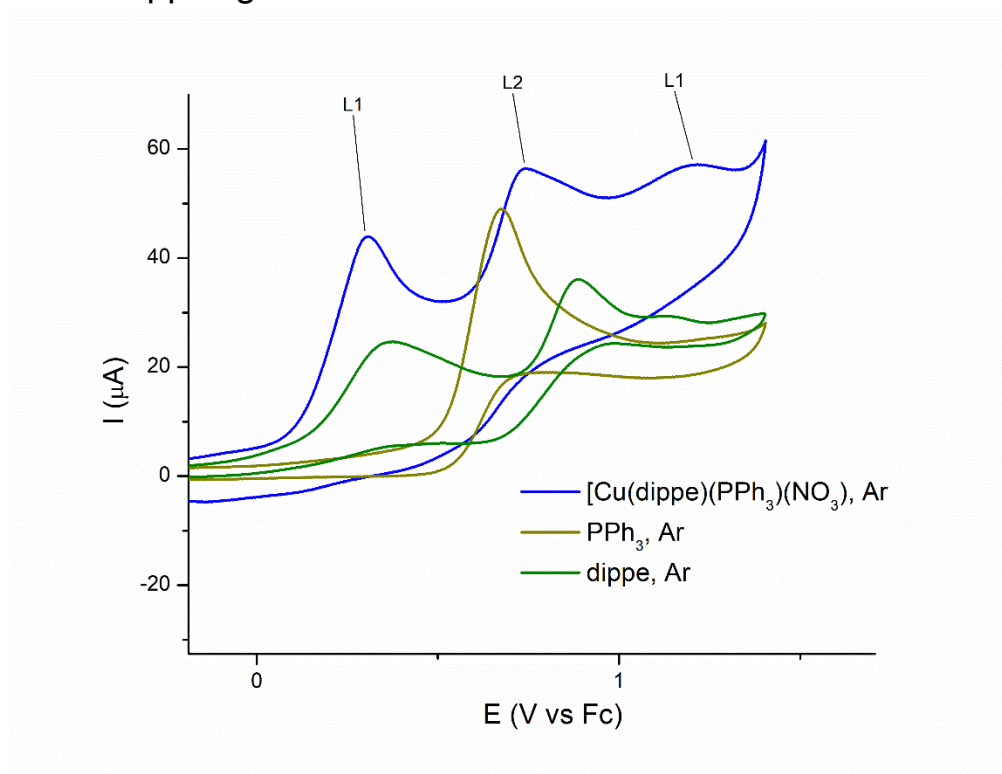


Figure S28. Anodic peaks assignments corresponding to phosphine ligands in compound (**2**)

For compound (3), L5 peak was assigned to the first oxidation of depe ligand. Anodic peak L2 + L5 corresponds to the sum of oxidation processes for PPh₃ and depe second oxidation process.

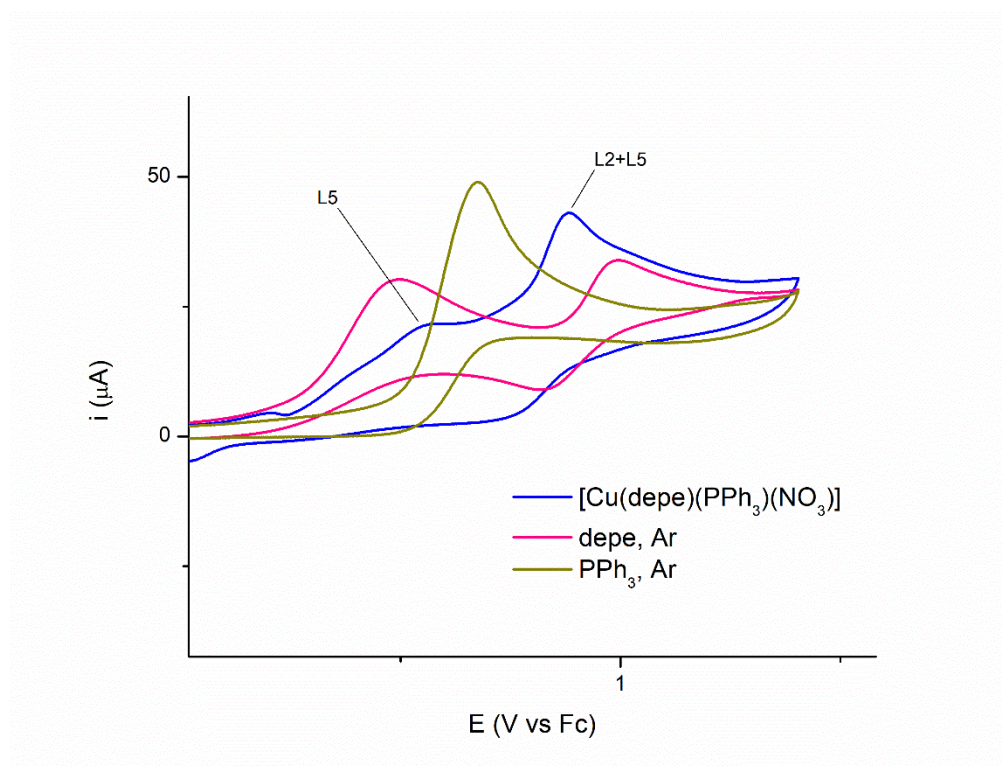


Figure S29. Assignment of anodic peaks of the phosphine ligands for compound (3)

For compound (4), L2 peak was assigned to the oxidation processes for PPh₃ and L3 peak corresponds to the oxidation of DIPHOS.

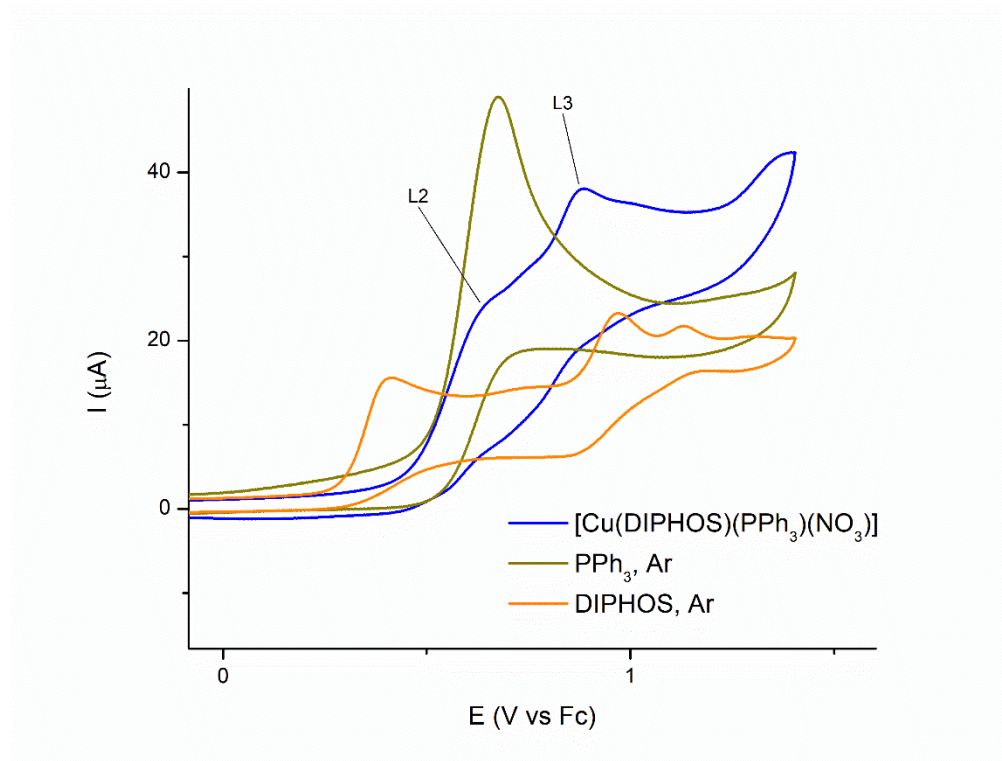


Figure S30. Assignment of anodic peaks of the phosphine ligands for compound (4)

Compound $[\text{Cu}(\text{dipf})\text{NO}_3]$ (**5**).

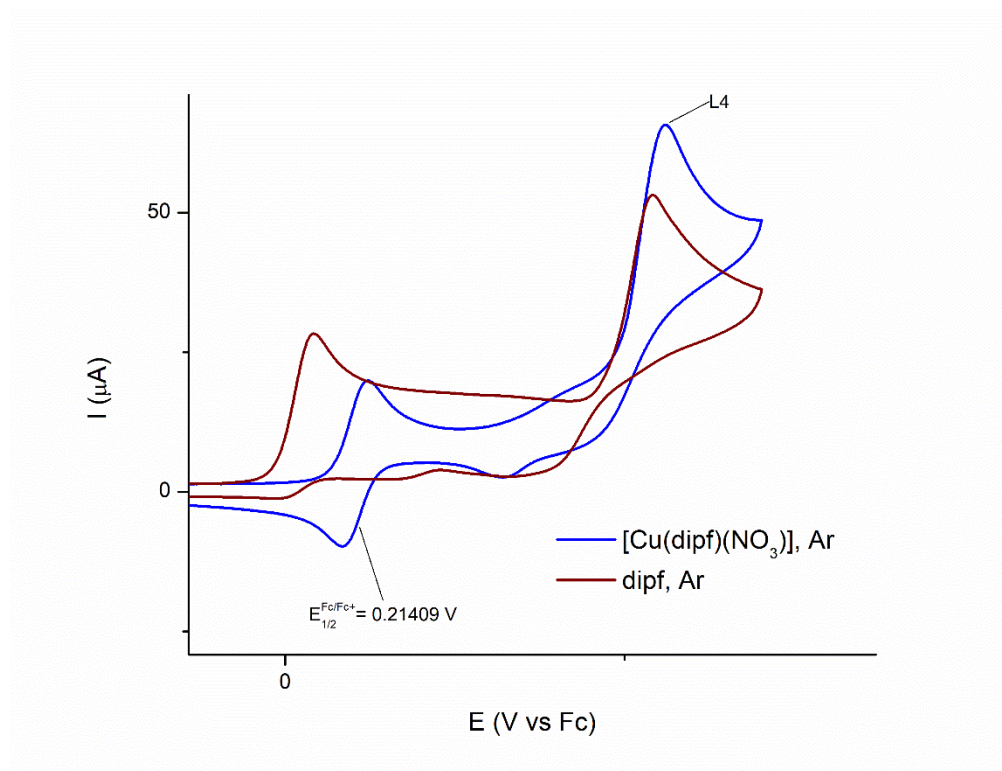


Figure S31. Assignment of anodic peaks of the phosphine ligands for compound (**5**)

L4 peak corresponds to the oxidation of dipf ligand, in Compound (**5**),

COMPOUND (2) BEHAVIOR UNDER Ar AND CO₂ ATMOSPHERE AND DIFFERENT PROTIC MEDIA.

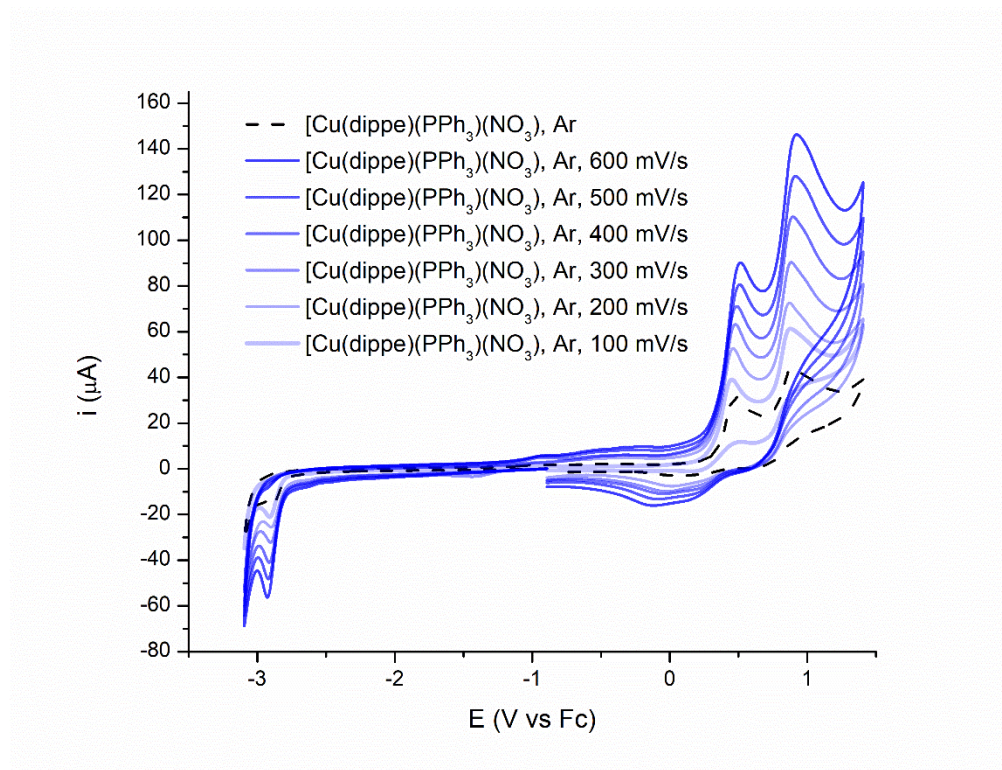


Figure S32. Compound (2) behavior with different scanning speeds in Ar atmosphere

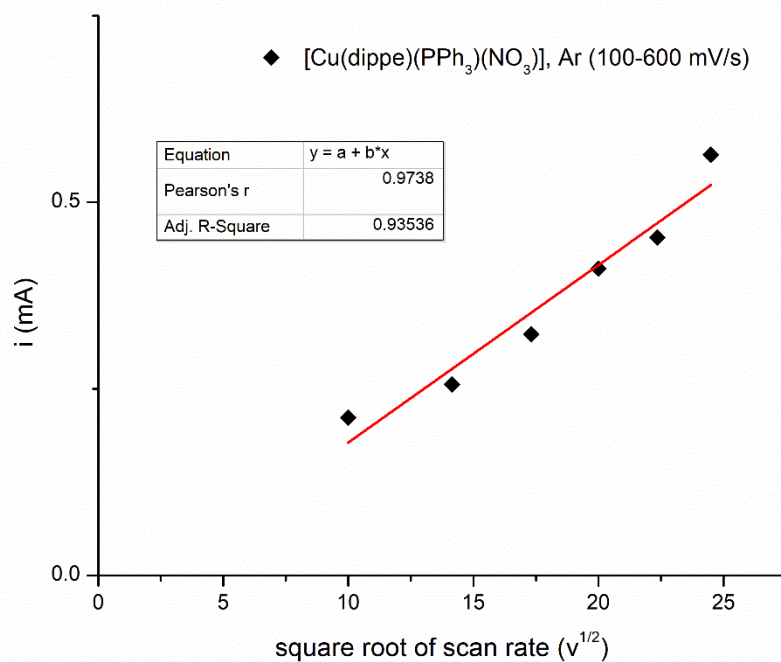


Figure S33. Pseudo-first-order behavior of the cathodic process of Compound (2)

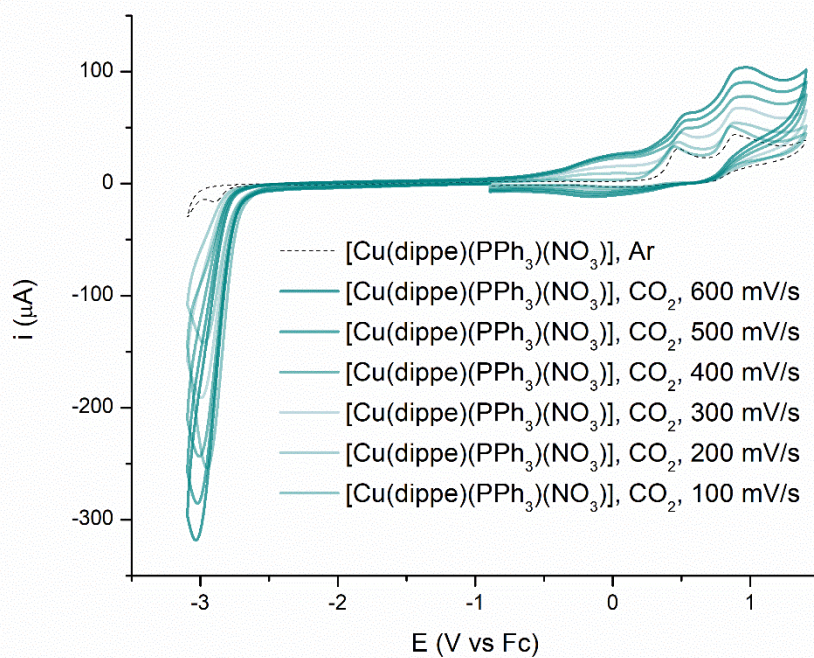


Figure S34. Compound (2) behavior with different scanning speeds in CO₂ atmosphere

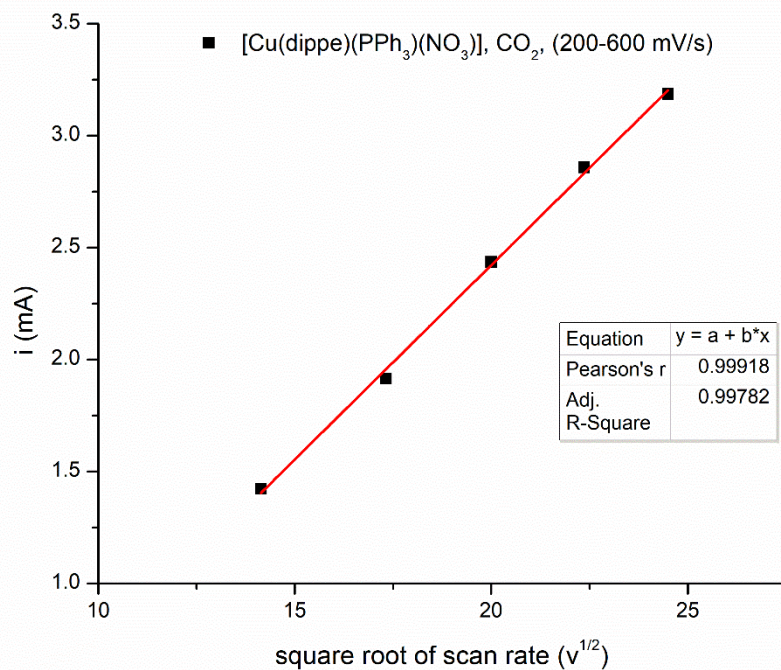


Figure S35. Pseudo-first-order behavior of the cathodic process of Compound (**2**) with CO₂.

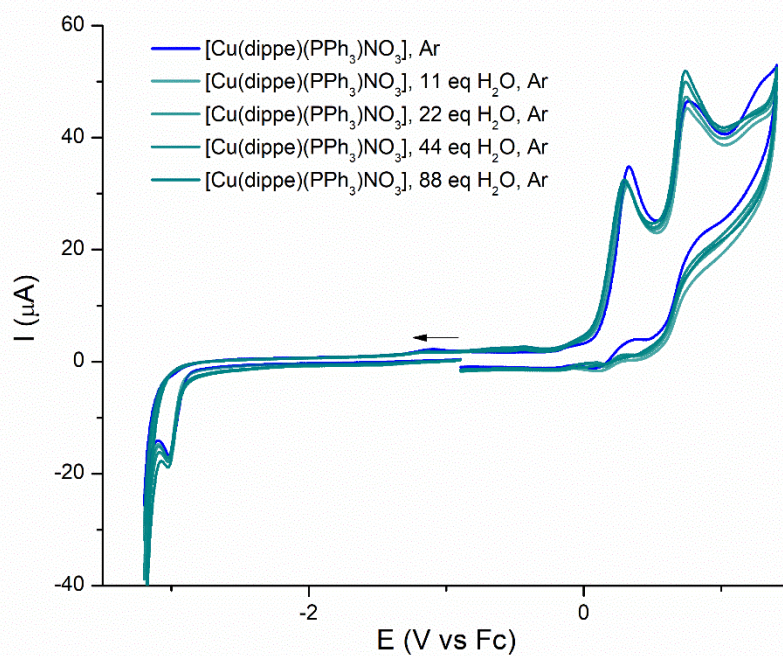


Figure S36. Compound (**2**) behavior with variable water equivalents under Ar atmosphere.

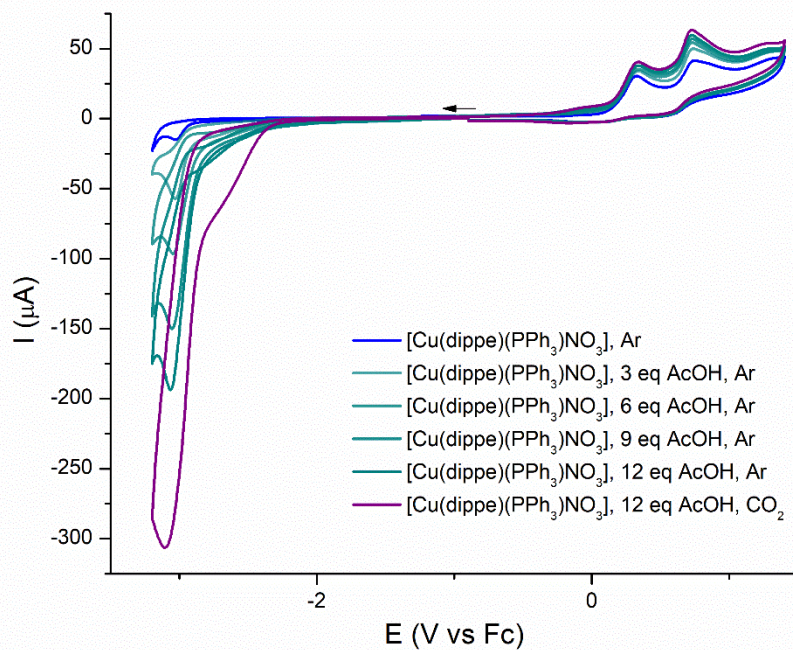


Figure S37. Compound (2) behavior with variable acetic acid equivalents under Ar and CO_2 atmosphere.

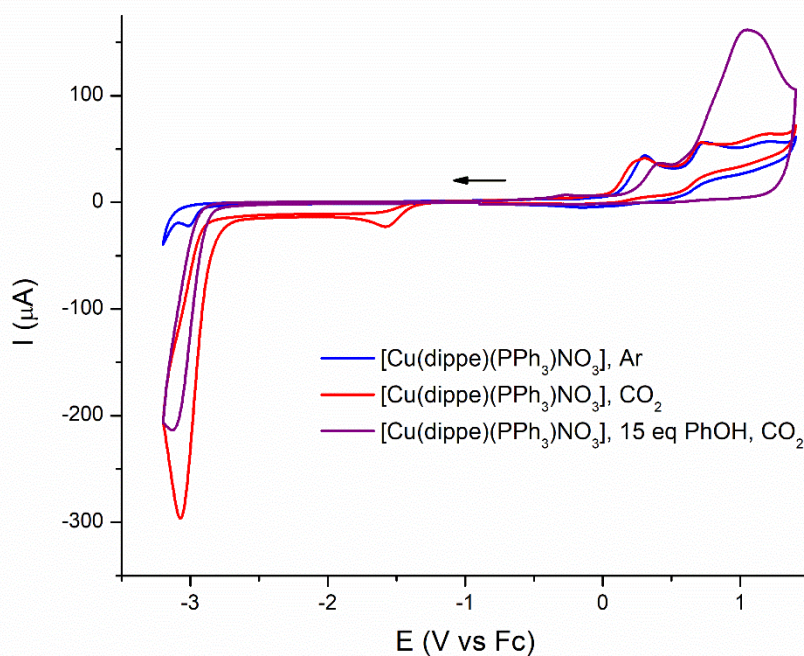


Figure S38. Compound (2) behavior with variable phenol equivalents and inhibition of the CO_2 RR process.

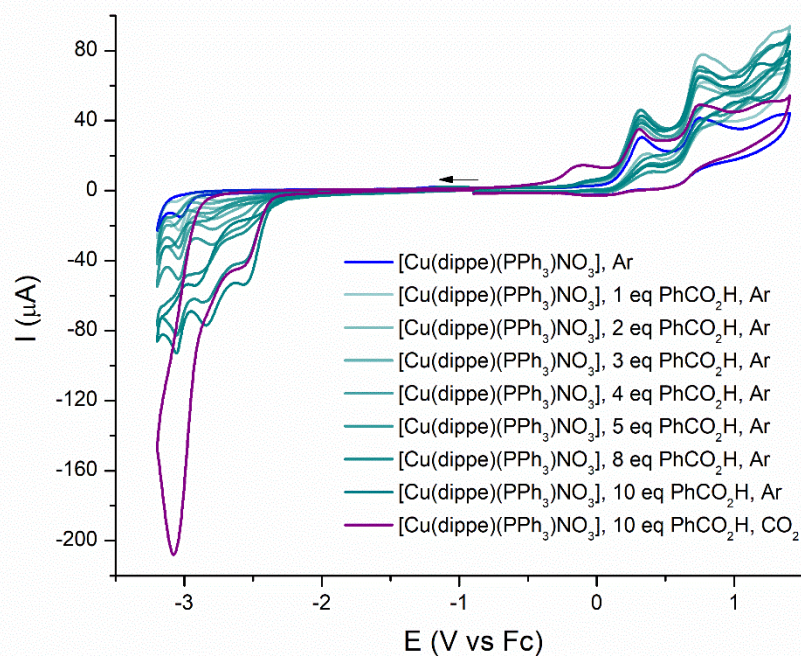


Figure S39. Compound (**2**) behavior with variable benzoic acid equivalents under Ar and CO₂ atmosphere.

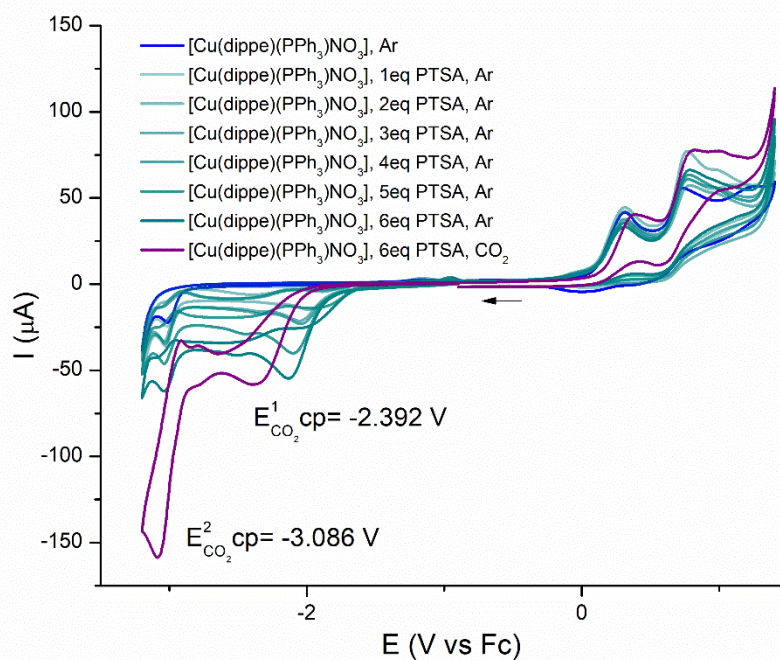


Figure S40. Compound (**2**) behavior with PTSA equivalents under Ar and CO₂ atmosphere.

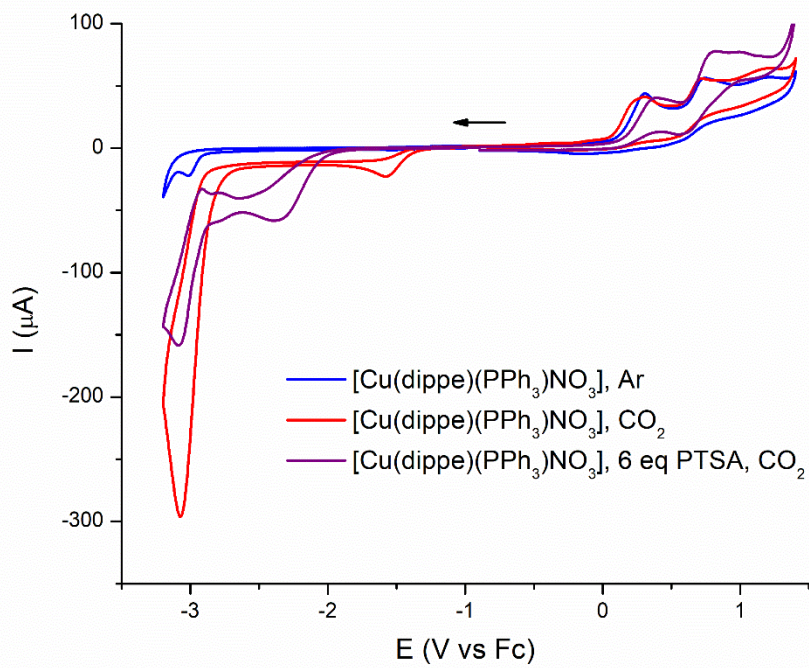


Figure S41. Compound (**2**) behavior with PTSA equivalents and inhibition of the CO_2RR process.

Compound (1), $[\text{Cu}(\text{PPh}_3)_2\text{NO}_3]$.

COMPOUND (1) BEHAVIOR UNDER Ar AND CO₂ ATMOSPHERE AND DIFFERENT PROTIC MEDIA.

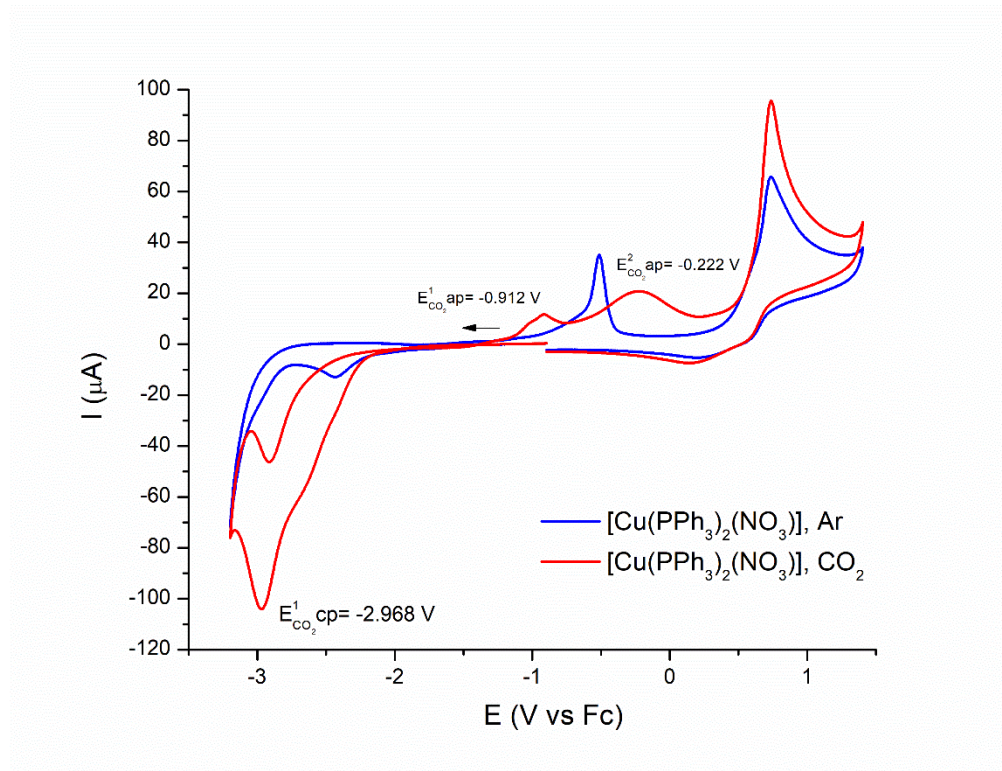


Figure S42. Compound (1) under Ar and CO₂ atmosphere.

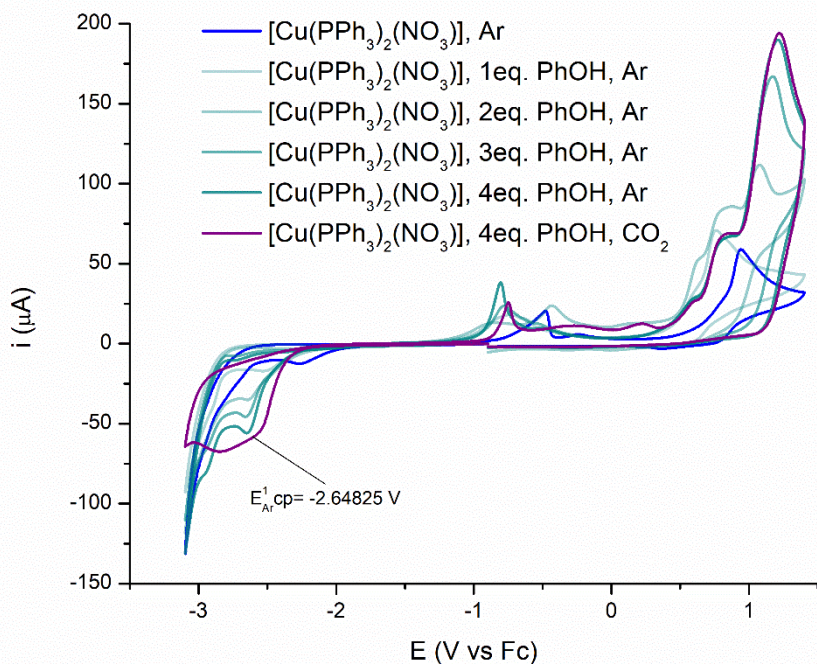


Figure S43. Compound (1) behavior with variable phenol equivalents under Ar and CO₂ atmosphere.

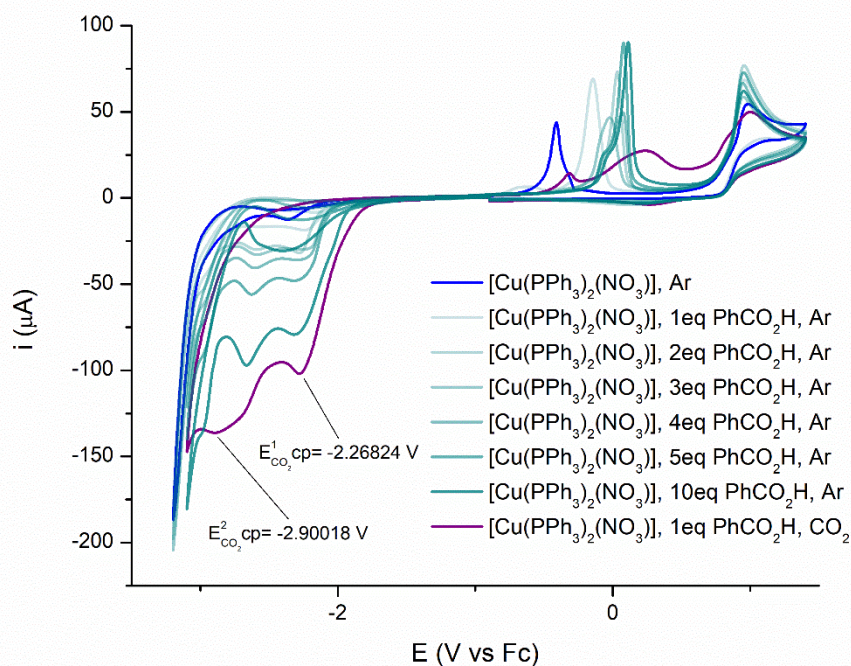


Figure S44. Compound (1) behavior with variable benzoic acid equivalents under Ar and CO₂ atmosphere.

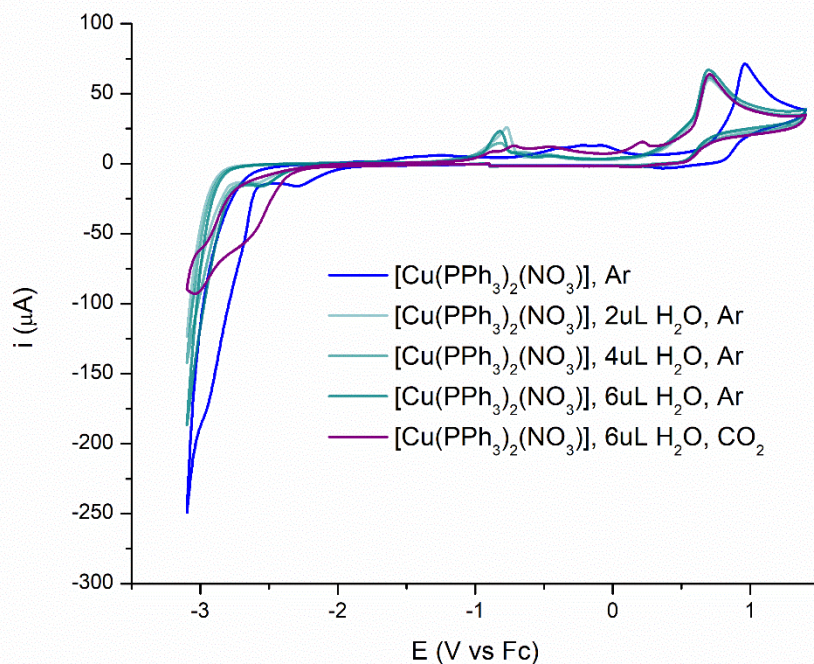


Figure S45. Compound (1) behavior with variable water equivalents under Ar and CO_2 atmosphere.

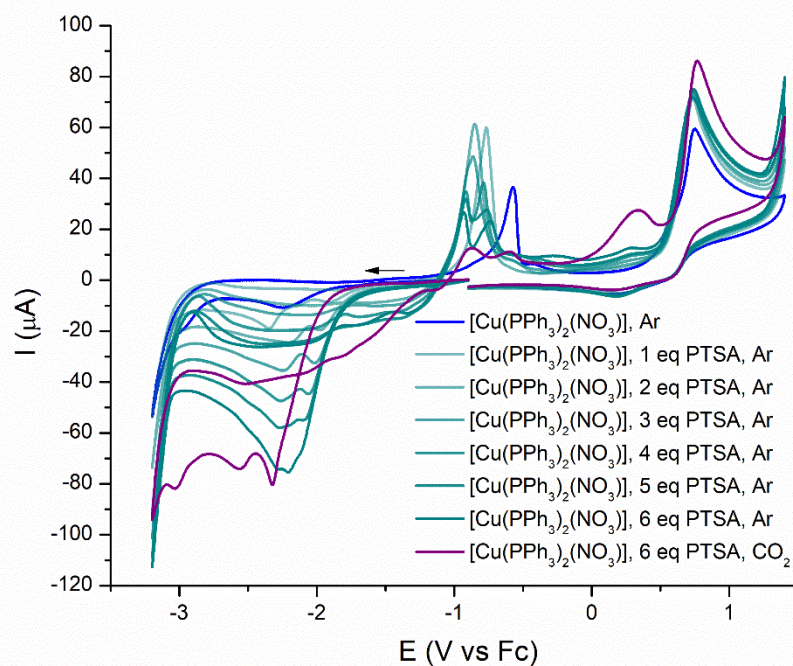


Figure S46. Compound (1) behavior with variable PTSA equivalents under Ar and CO_2 atmosphere.

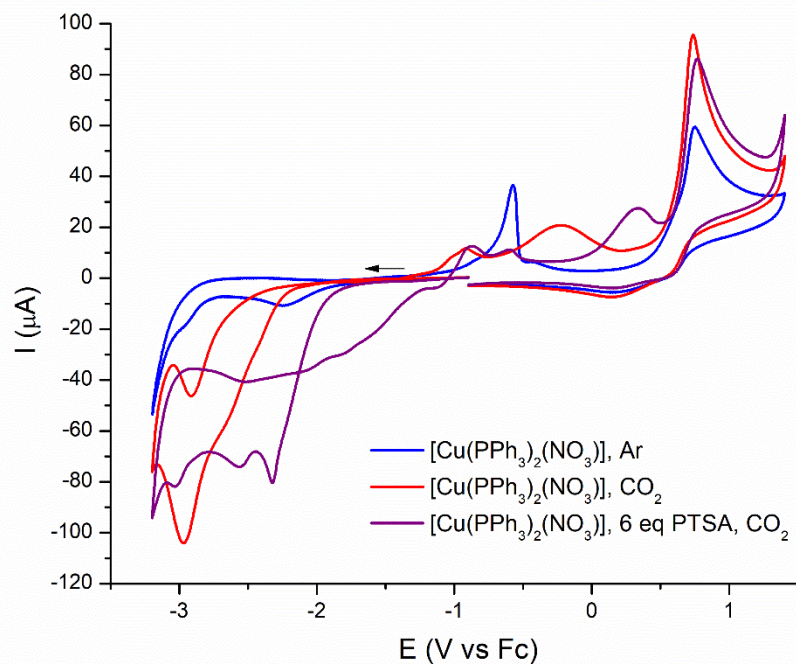


Figure S47. Compound (1) behavior with variable PTSA equivalents and inhibition of the CO_2RR process.

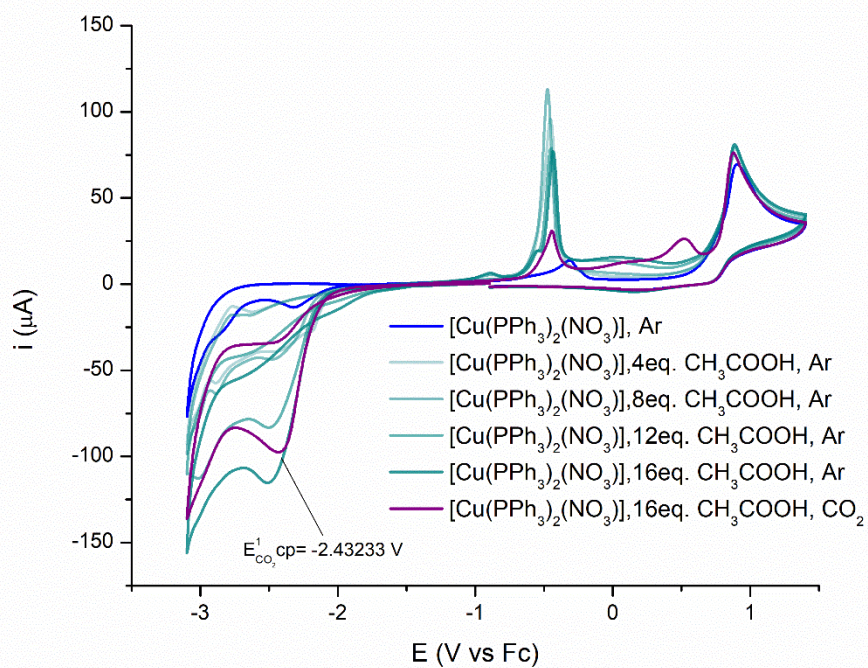


Figure S48. Compound (1) behavior with variable acetic acid equivalents under Ar and CO_2 atmosphere.

Compound (3), [Cu(depe)(PPh₃)(NO₃)].

**COMPOUND (3) BEHAVIOR UNDER Ar AND CO₂ ATMOSPHERE,
AND DIFFERENT PROTIC MEDIA.**

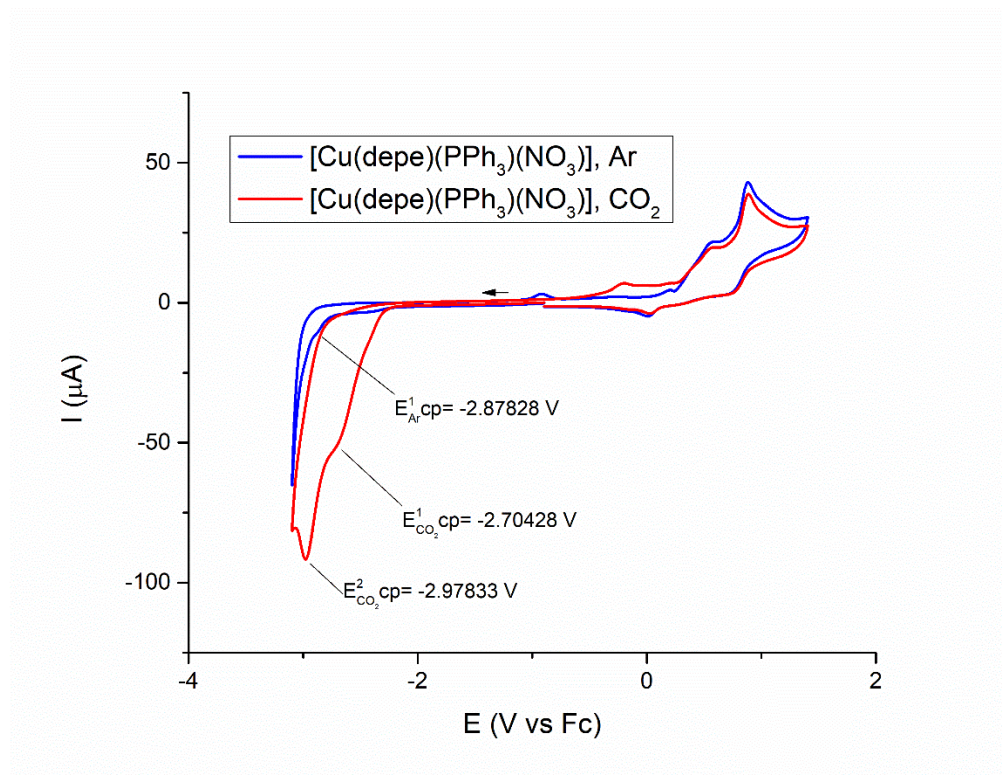


Figure S49. Compound (3) under Ar and CO₂ atmosphere.

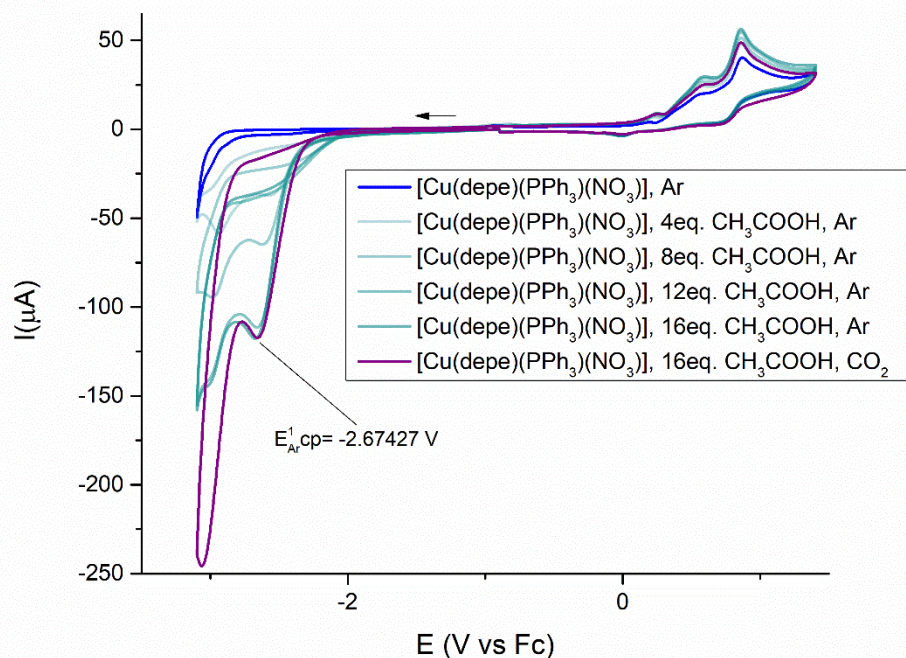


Figure S50. Compound **(3)** behavior with variable acetic acid equivalents under Ar and CO₂ atmosphere.

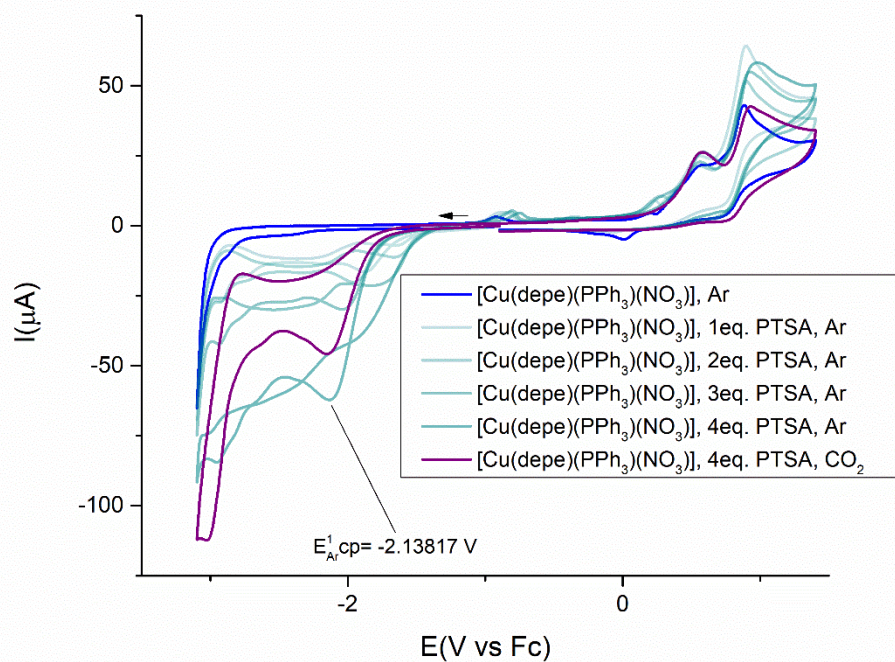


Figure S51. Compound **(3)** behavior with variable PTSA equivalents under Ar and CO₂ atmosphere.

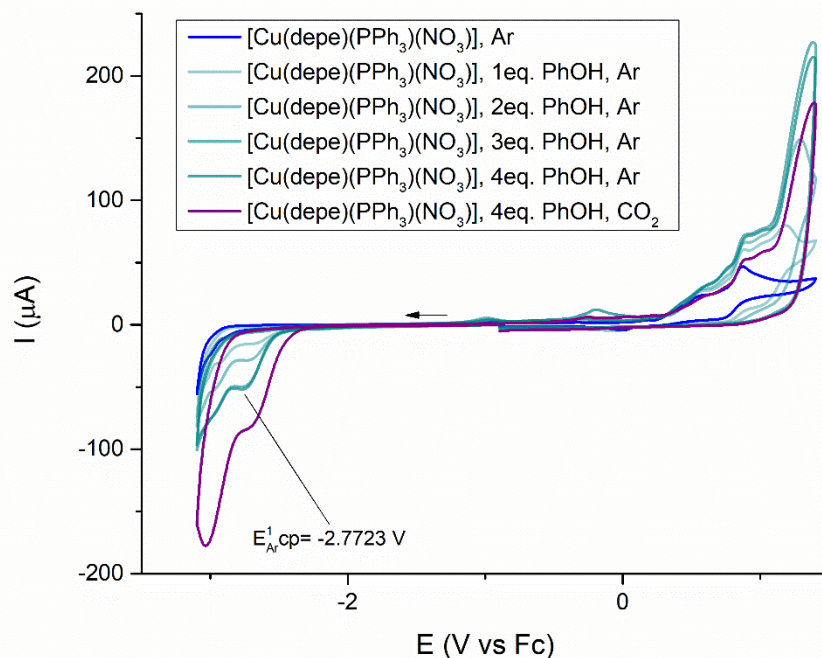


Figure S52. Compound (3) behavior with variable phenol equivalents under Ar and CO₂ atmosphere.

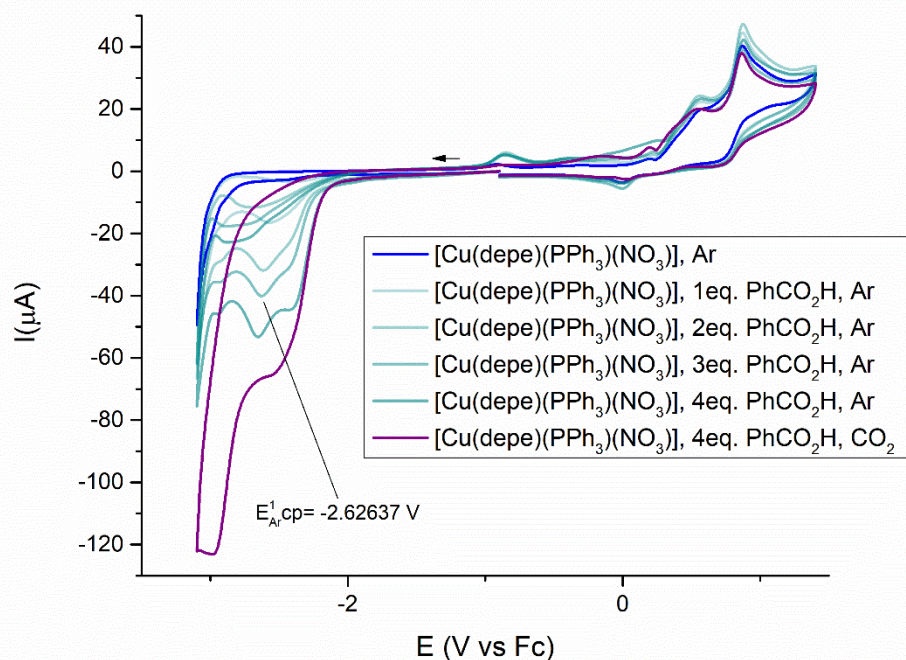


Figure S53. Compound (3) behavior with variable benzoic acid equivalents under Ar and CO₂ atmosphere.

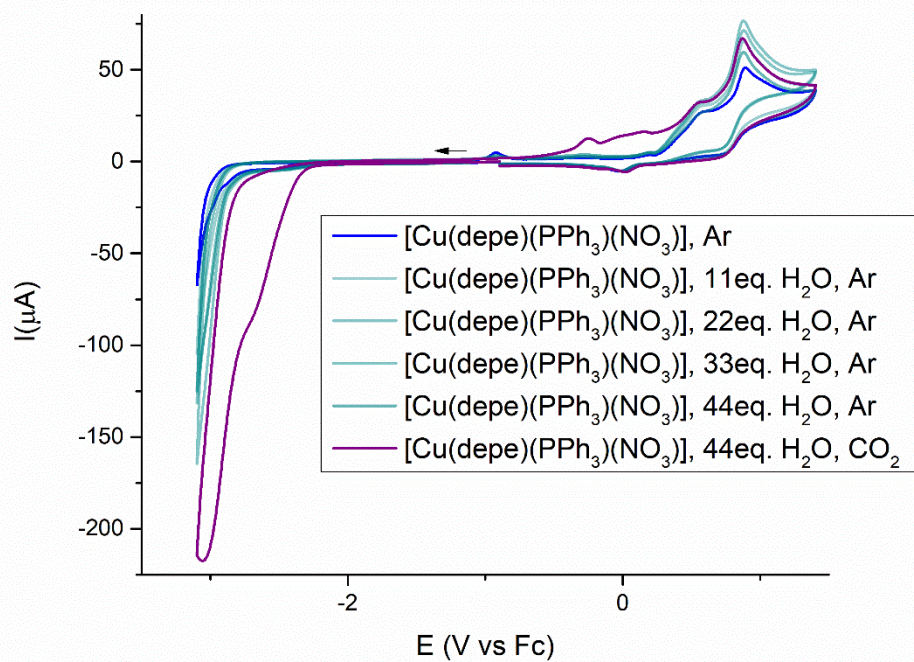


Figure S54. Compound (3) behavior with variable water equivalents under Ar and CO₂ atmosphere.

Compound (4), [Cu(dppe)(PPh₃)(NO₃)].

**COMPOUND (4) BEHAVIOR UNDER Ar AND CO₂ ATMOSPHERE,
AND DIFFERENT PROTIC MEDIA.**

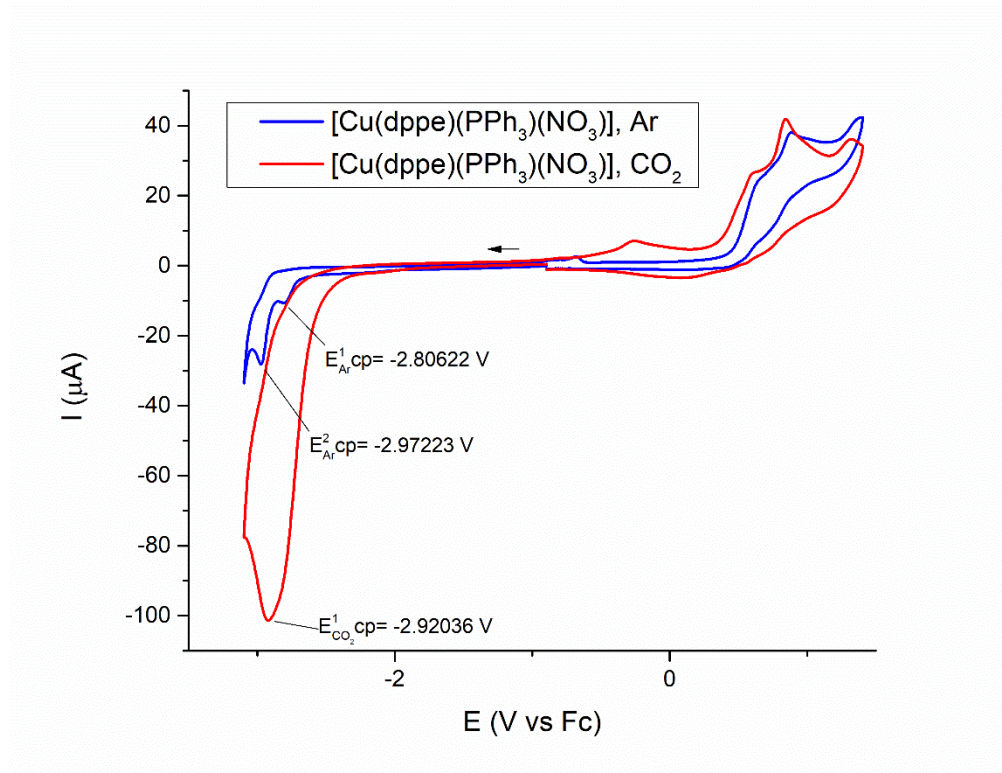


Figure S55. Compound (4) under Ar and CO₂ atmosphere.

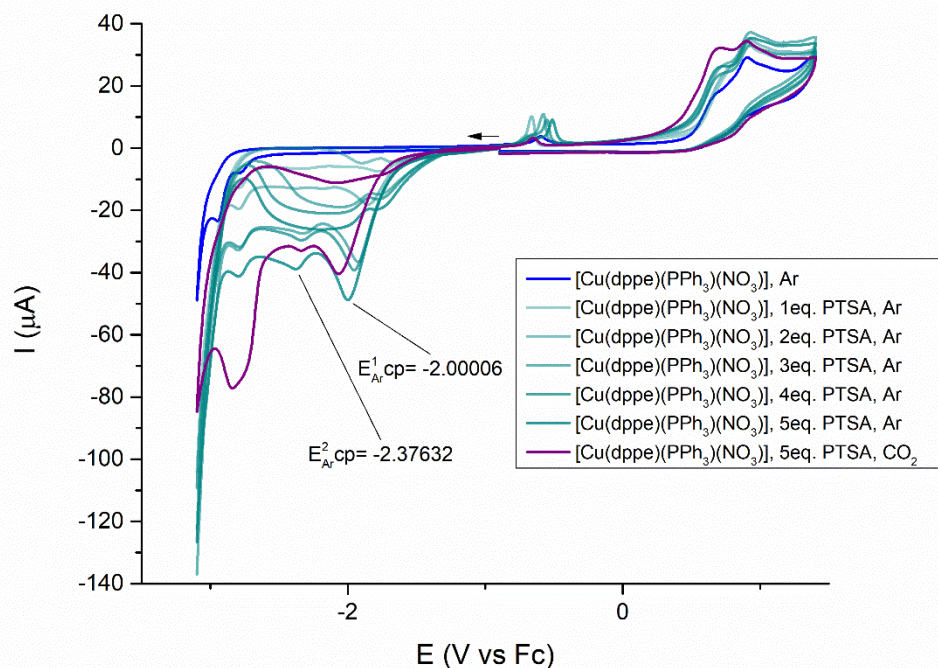


Figure S56. Compound (4) behavior with variable PTSA equivalents under Ar and CO₂ atmosphere.

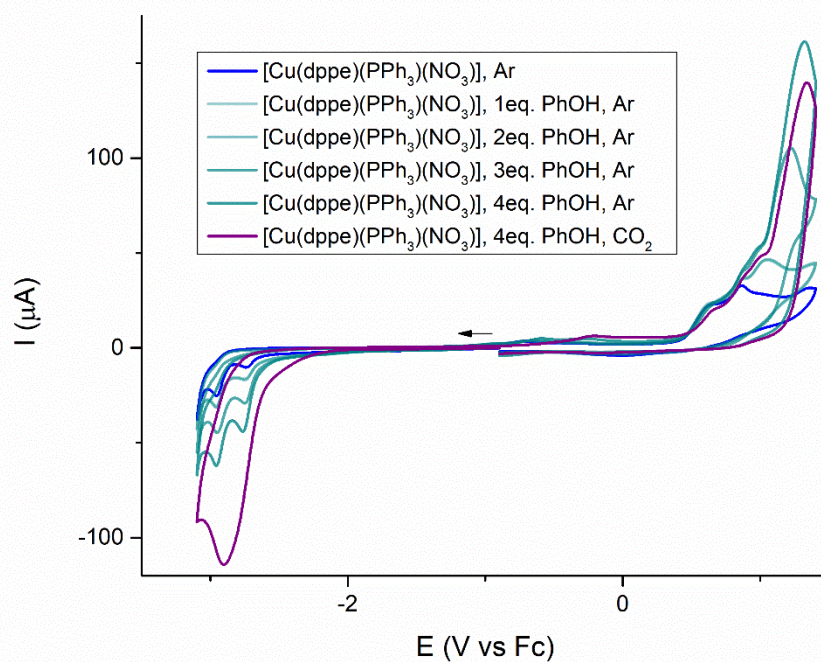


Figure S57. Compound (4) behavior with variable phenol equivalents under Ar and CO₂ atmosphere.

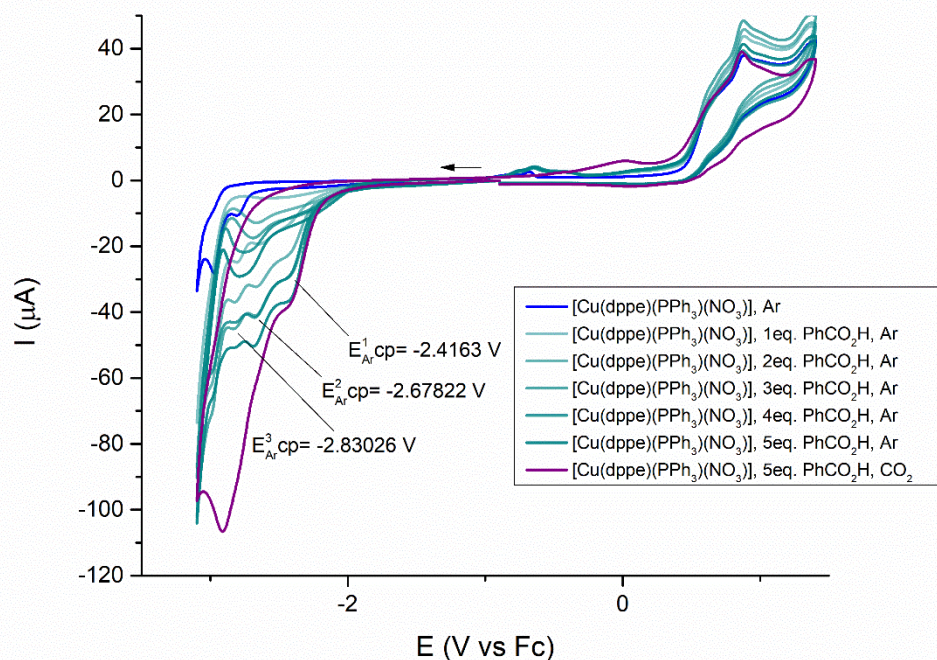


Figure S58. Compound (**4**) behavior with variable benzoic acid equivalents under Ar and CO₂ atmosphere.

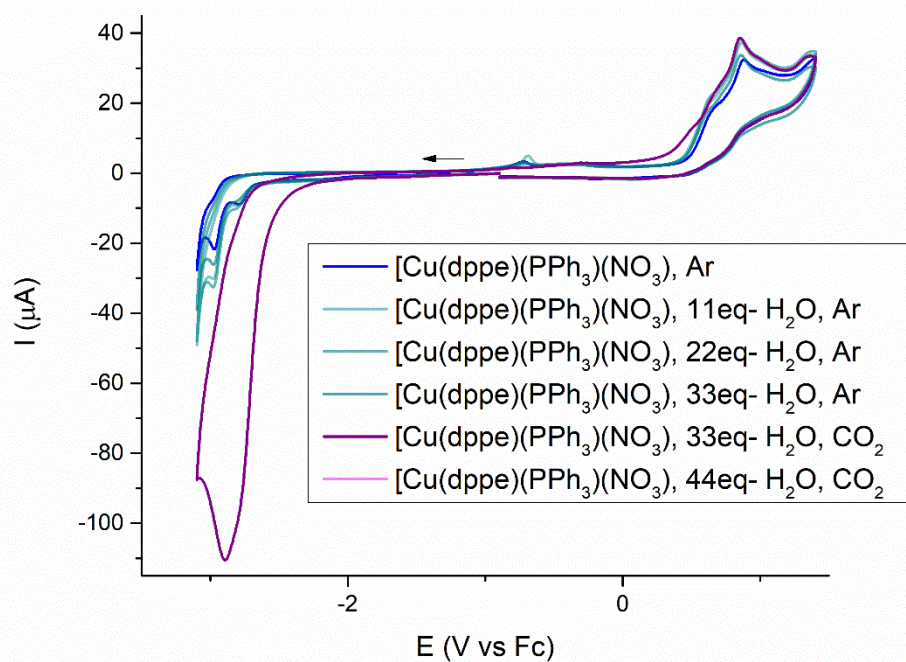


Figure S59. Compound (**4**) behavior with variable water equivalents under Ar and CO₂ atmosphere.

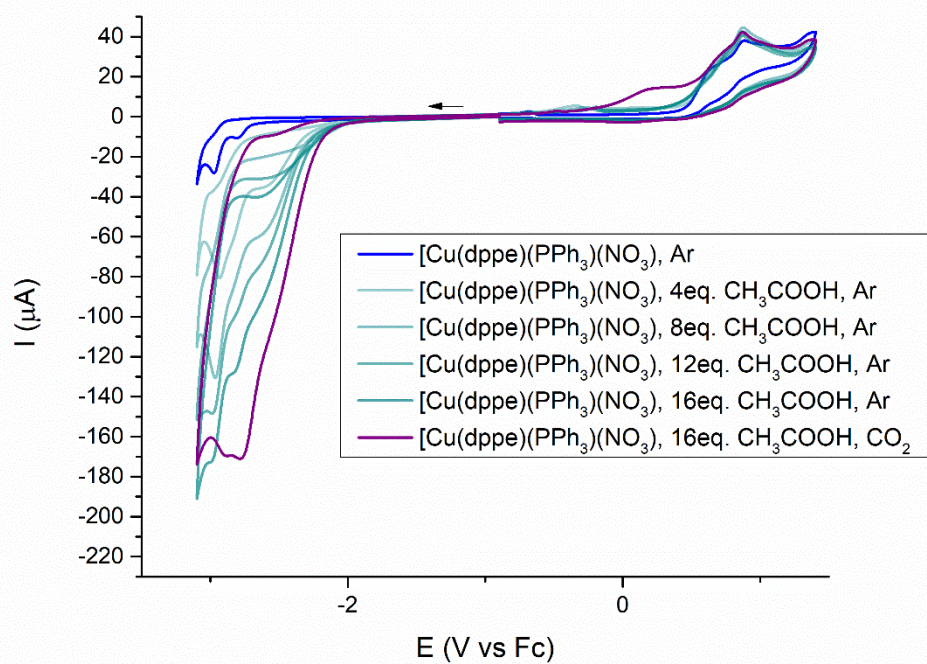


Figure S60. Compound (4) behavior with variable acetic acid equivalents under Ar and CO_2 atmosphere.

Compound (5), [Cu(dippf)NO₃].

**COMPOUND (5) BEHAVIOR UNDER Ar AND CO₂ ATMOSPHERE,
AND DIFFERENT PROTIC MEDIA.**

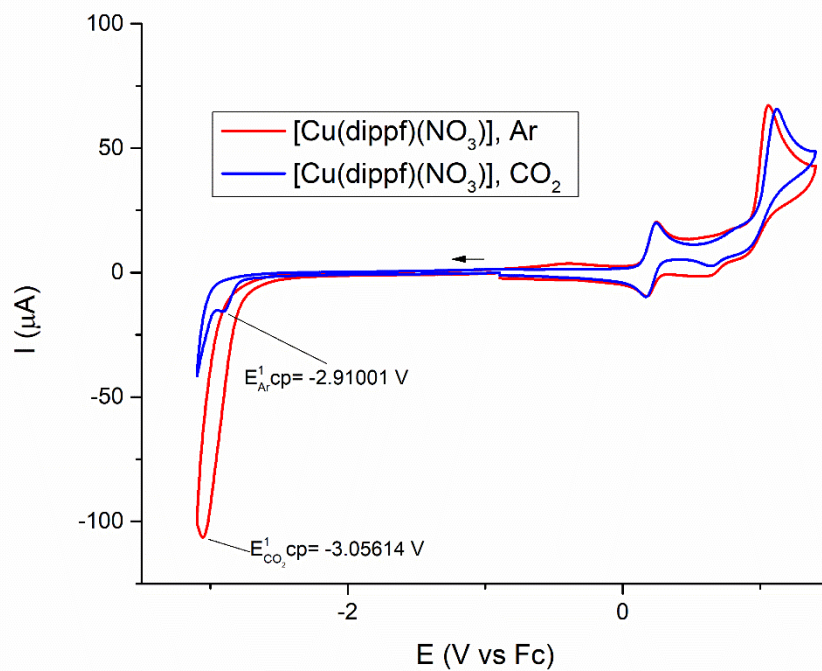


Figure S61. Compound (5) under Ar and CO₂ atmosphere.

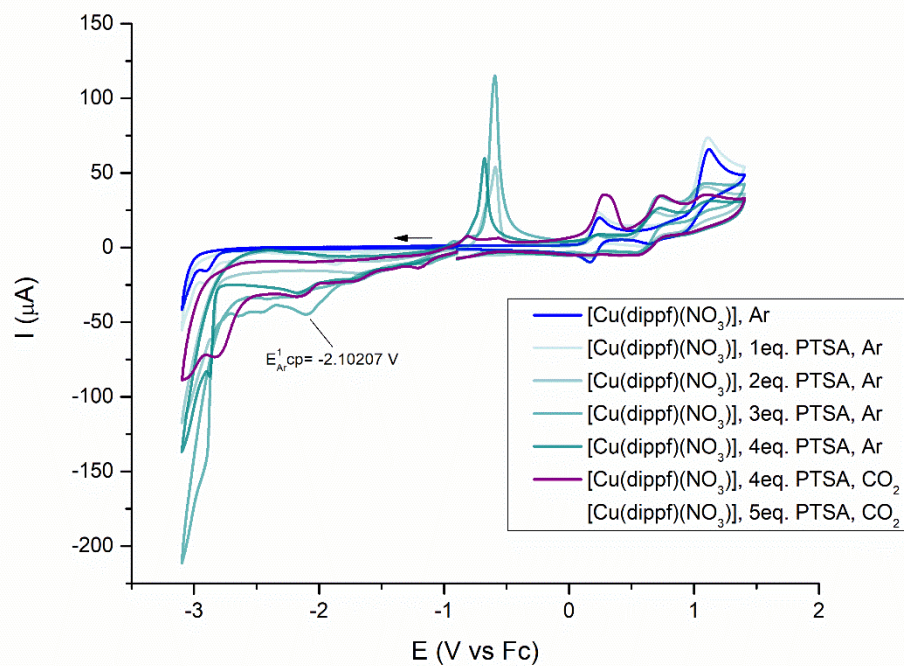


Figure S62. Compound (5) behavior with variable PTSA equivalents under Ar and CO₂ atmosphere.

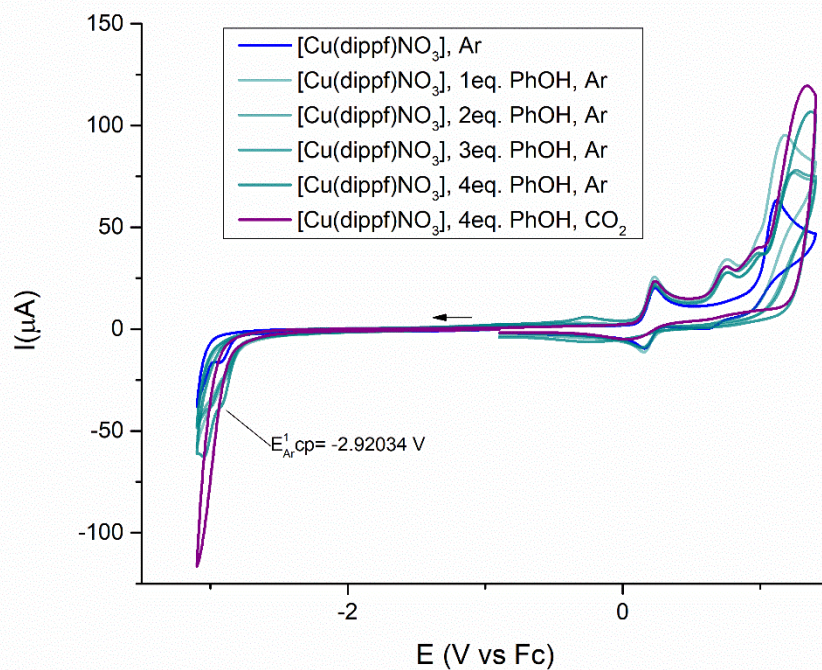


Figure S63. Compound (5) behavior with variable phenol equivalents under Ar and CO₂ atmosphere.

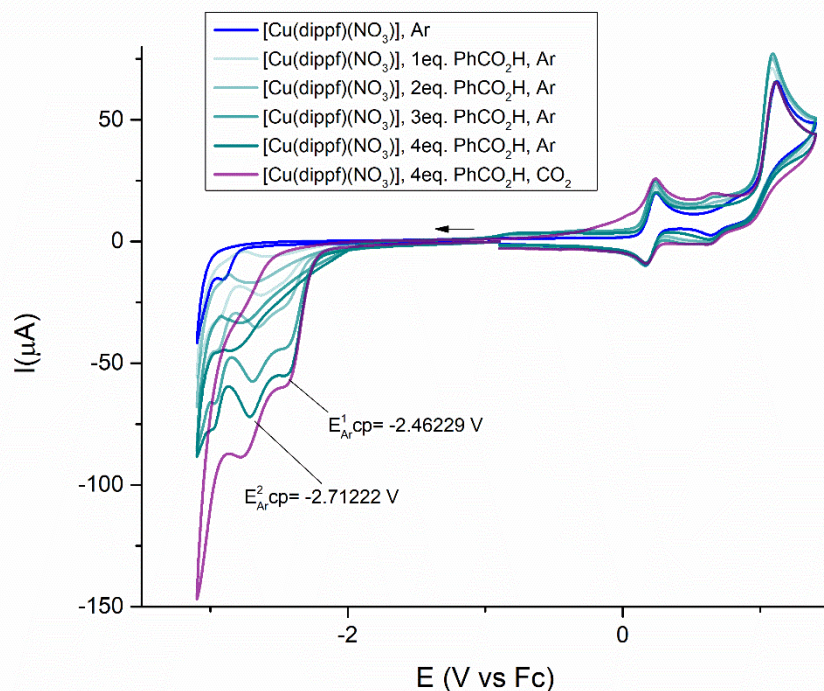


Figure S64. Compound (**5**) behavior with variable benzoic acid equivalents under Ar and CO₂ atmosphere.

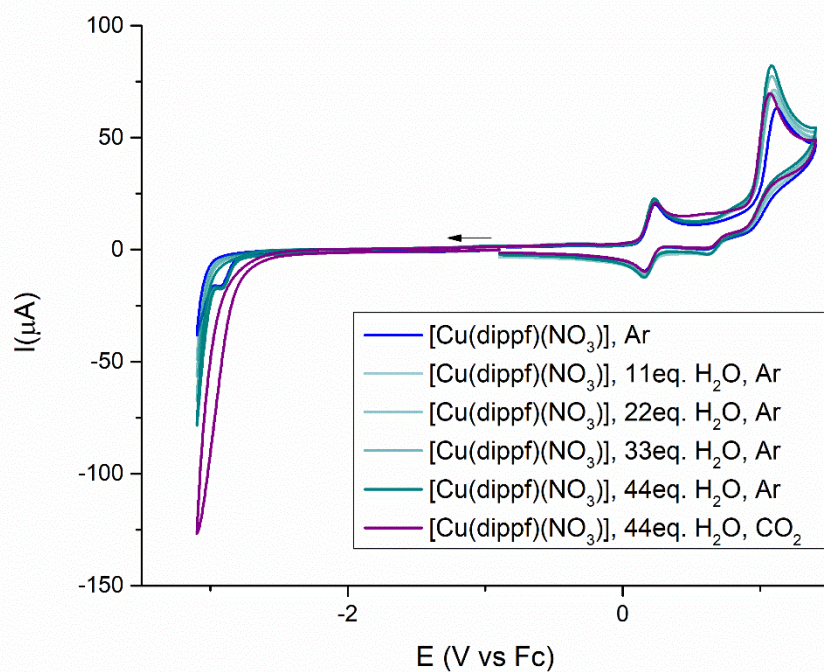


Figure S65. Compound (**5**) behavior with variable water equivalents under Ar and CO₂ atmosphere.

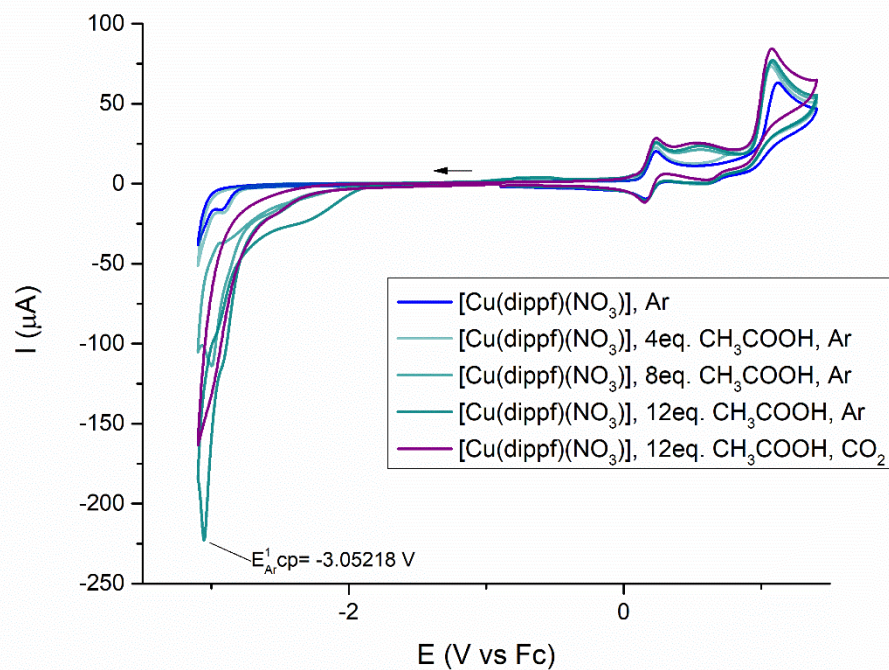


Figure S66. Compound (5) behavior with variable acetic acid equivalents under Ar and CO₂ atmosphere.

Unidad de Servicios de Apoyo a la Investigación y a la Industria (USAI)
 Facultad de Química, UNAM, Edificio H "Mario Molina"
 Email: viclemus@unam.mx
 Phone: 56.22.38.99 Ext. 84040

| | |
|-----------------------|-----------------------------------------|
| Date of report | 22-May-23 7:05:48PM |
| User ID | Realizo: M en I. Victor Hugo Lemus Neri |
| Comments | Muestra: AA507CPCW |

| Run | Weight | Carbon | Hydrogen | Nitrogen | Created on |
|-------------|--------------------------|--------|----------|----------|----------------------|
| 4423055320B | 1.655 | 67.81% | 5.21% | 1.38% | 22-May-23 4:49:12 PM |
| 4423055320A | 1.341 | 67.75% | 5.26% | 1.56% | 22-May-23 4:44:08 PM |
| | Weight | Carbon | Hydrogen | Nitrogen | |
| | Average 1.498 | 67.780 | 5.235 | 1.470 | |
| | Variance 0.049 | 0.002 | 0.001 | 0.016 | |
| | Standard Deviation 0.222 | 0.042 | 0.035 | 0.127 | |

Figure S67. Elemental Analysis for $[\text{Rh}(\text{PPh}_3)_3\text{Cl}(\text{NO})]$.

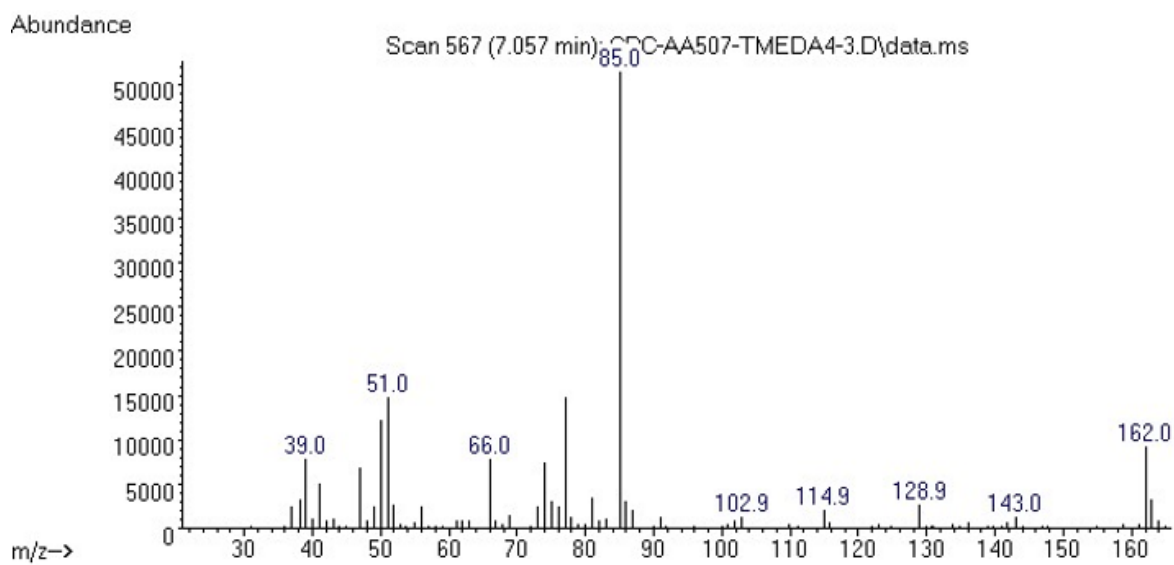


Figure S68. MS spectra of hydrolyzed product (d).
(m/z)= 162, 115 (2H, CO₂), 85 (-HNMe).